



1 Tree-ring stable isotopes for regional discharge reconstruction 2 in eastern Labrador and teleconnection with the Arctic Oscillation

3 Lauriane Dinis¹ · Christian Bégin¹ · Martine M. Savard¹ · Joëlle Marion¹ · Pierre Brigode² · Cristian Alvarez³

4 Received: 19 September 2018 / Accepted: 12 March 2019
5 © Crown 2019

6 Abstract

7 In northeastern Canada (Labrador), instrumental climatic data cover less than 70 years and long reconstructions from natural
8 archives are non-existent. This study specifically aims at helping filling this gap of knowledge by testing the possibility of
9 reconstructing the regional 1800–2009 discharge of the lower Churchill River from black spruce tree-ring $\delta^{13}\text{C}$ and $\delta^{18}\text{O}$
10 series. The results illustrate direct relationships of summer climatic variables/derived parameters (maximum temperature,
11 total precipitation and vapor pressure deficit) with tree-ring isotope values. Importantly, they show an inverse correlation
12 between tree-ring isotope values and regional river discharge due to common climate forcing. To a lesser extent, transpira-
13 tion also affects the river discharge and tree-ring isotopic compositions. The reconstructed river discharge series agrees
14 with an independent reconstruction based on the ANATEM method (1880–2009 period). The agreement between the two
15 reconstructions validates the two approaches for reconstructing regional hydroclimatic conditions at high latitudes. More-
16 over, the reconstructions suggest that summer discharge has decreased over the past 200 years in eastern Labrador and more
17 broadly at the Québec-Labrador peninsula scale. This trend correlates with the long-term summer Arctic Oscillation (AO)
18 that influences summer regional climatic conditions. This research contributes with other studies to build up observations
19 linking summer AO and eastern Canada climatic conditions, and calls for research on mechanisms explaining these relation-
20 ships during summer.

21 **Keywords** Past discharge reconstruction · Carbon isotopes · Oxygen isotopes · Tree rings · Arctic Oscillation · Labrador

22 1 Introduction

23 Impacts of climate change on global hydrological regimes
24 exert great pressure on water resources, and in several
25 areas of the world, adaptation represents one of the big-
26 gest socio-economic challenges of the twenty-first century.
27 This is the case in Canada, the second largest generator of

hydroelectricity in the world, with 60% of its power coming
from river dams. Consequently, the hydropower industry in
this country needs understanding the natural variations in
surficial water resources (Natural Resources and Canada
2018). Zhang et al. (2001) have shown that modification of
precipitation, temperature, snowpack and potential evapo-
transpiration have significantly influenced annual river dis-
charge with a general decrease across Canada during the
last century. However, predictions of streamflow through
modelling differ from a region to another, with an annual
decrease in the Prairies, an increase in New Brunswick, Lab-
rador and northern Canada, and a mixed trend in Yukon,
Ontario and Quebec (Cohen et al. 2015; Déry et al. 2009;
Mortsch et al. 2015; Roberts et al. 2012; Rood et al. 2005,
St. George 2007). It seems that large-scale atmospheric and
oceanic variability modes influence seasonal climate, which
in turn modifies annual river discharge in various Canadian
regions (Bonsal and Shabbar 2008). For example, telecon-
nection between winter atmospheric large-scale circula-
tion such as the North Atlantic Oscillation (NAO) and the

28
29
30
31
32
33
34
35
36
37
38
39
40
41
42
43
44
45
46
47

A1 **Electronic supplementary material** The online version of this
A2 article (<https://doi.org/10.1007/s00382-019-04731-2>) contains
A3 supplementary material, which is available to authorized users.

A4 ✉ Lauriane Dinis
A5 lauriane.dinis@canada.ca

A6 ¹ Geological Survey of Canada, Natural Resources Canada,
A7 490 rue de la Couronne, Québec, QC G1K 9A9, Canada

A8 ² Université Côte d'Azur, CNRS, OCA, IRD, Géoazur, Nice,
A9 France

A10 ³ Centre Eau Terre Environnement, Institut national de la
A11 recherche scientifique, 490 rue de la Couronne, Québec,
A12 QC G1K 9A9, Canada

Arctic Oscillation (AO) indices with yearly river discharge and groundwater have been observed in northeastern Canada (Antil and Coulibaly 2004; Bonsal and Shabbar 2008; Coulibaly et al. 2000; Coulibaly and Burn 2005; Déry et al. 2009; Nicault et al. 2014; Tremblay et al. 2011). During a positive phase of NAO and AO, winter precipitation are lower than normal, hence reducing annual streamflow (Bonsal and Shabbar 2008).

Hydrological models are developed from instrumental hydroclimatic data series, which are generally discontinued, scarce or short (40–50 years). This short coverage limits (1) examining past natural river variations, (2) optimizing model calibration, and (3) predicting recurrence of extreme events. In other words, simulating hydroclimatic variabilities and estimating future drought risks are tasks destined to very limited success if longer series are not available. Paleoclimate proxies such as ice cores, peat deposits, marine and lake sediments, speleothems and tree ring have the potential to compensate for the lack of direct measurements by extending climatic series back in time. During their formation, paleoclimate proxies are modulated by climatic conditions, so that they provide an indirect record of climatic variables at various time scales. Trees under temperate conditions offer the advantage of an absolute dating at annual or sub-annual resolution, are widely distributed and can provide several-century long series of climate proxies. Among the different existing tree-ring indicators, ring width have been extensively used to reconstruct streamflow in arid, semi-arid and temperate regions (e.g., Axelson et al. 2009; Case and MacDonald 2003; Coulthard and Smith 2016; Elshorbagy et al. 2016; Hart et al. 2010; Sauchyn et al. 2015; Stockton and Fritts 1973; Woodhouse and Lukas 2006). However, ring width series have to be corrected for tree age-dependent biological growth trends using statistical detrending methods prior to infer any climatic signal. Depending on the detrending model, low-frequency information related to climate variability can be potentially lost (Sullivan et al. 2016). Tree-ring carbon ($\delta^{13}\text{C}$) and oxygen ($\delta^{18}\text{O}$) isotope series require analytical efforts differing from traditional tree-ring investigations, and they provide complementary information as biogeochemical processes influenced by ambient conditions and responsible for modifying variations in both proxies slightly differ (Naulier et al. 2015a). In general, they also present the advantage of not needing to be corrected for developmental effects. Nonetheless, some studies have reported that, in some cases, physiological processes such as tree age, size and height could influence tree-ring isotope composition (Brienen et al. 2017; Marshall and Monserud 2006; Treydte et al. 2006). During carbon assimilation by trees, gaseous diffusion and carboxylation are the first processes that modulate tree-ring $\delta^{13}\text{C}$ values. Those mechanisms discriminate against the heavy carbon isotope (^{13}C) modifying the CO_2 $\delta^{13}\text{C}$ values from

–8‰ in the atmosphere to –27‰ in leaves (Farquhar et al. 1989). Thus, carbon isotopic fractionation is defined by the following equation (Farquhar et al. 1982):

$$\delta^{13}\text{C}_{\text{plant}} = \delta^{13}\text{C}_{\text{atm}} - a - (b - a)(c_i/c_a) \quad (1)$$

where a represents the discrimination against ^{13}C during diffusion, b the discrimination against ^{13}C associated with carboxylation, and where c_i and c_a are the intercellular and ambient CO_2 concentrations, respectively. As to tree-ring $\delta^{18}\text{O}$ values, they mainly reflect three processes: (1) assimilation of source water imprinted by precipitation signals possibly mixed with stationary soil water; (2) transpiration enriching and Péclet effect depleting needle water; and (3) biochemical fractionation during the synthesis of organic matter (Anderson et al. 2002; Barbour 2007; Ferrio and Voltas 2005; Gazis and Feng 2004; Roden et al. 2000). The latter process should stay constant through time (Leuenberger 1998) whereas water uptake by roots should not cause any fractionation (Wershaw et al. 1966). Therefore, several studies have used the climatic signal contained in tree-ring $\delta^{13}\text{C}$ and $\delta^{18}\text{O}$ values of α -cellulose to reconstruct temperature and precipitation over centuries or millennia (Bégin et al. 2015; Csank et al. 2013; Hook et al. 2015; Naulier et al. 2015a; Porter et al. 2014).

To our knowledge, up to now only two studies have used tree-ring isotopes to reconstruct streamflow variations (Waterhouse et al. 2000; Wils et al. 2010). Waterhouse et al. (2000) observed a highly significant inverse correlation between river flow and scots pine $\delta^{13}\text{C}$ values during growing season in western Siberia. They invoked a moisture transferred from river to trees through air which influences stomatal aperture and hence tree-ring $\delta^{13}\text{C}$ values. They also show that the strength of the relationship is distance-dependant, as trees at the river edge had higher correlations than trees 60 m away. Wils et al. (2010) found a significant negative correlation between the isotopic series from African pencil cedar trees and river flow of the previous dry season in Ethiopia. They argued that river flow reflects plant water availability. During the previous dry season, increase in water stress reduced the amount of needles for the next growing season. The available resources (water and nutrients) are thus diverted to the remaining needles, increasing needle-level photosynthetic rate and consequently the $\delta^{13}\text{C}$ values.

The province of Newfoundland and Labrador is the fourth most important producer of hydroelectricity in Canada, with the Churchill Falls hydroelectricity generating station in Labrador producing about 5400 of 7400 MW for the province (Government of Newfoundland Labrador 2018a). The longest instrumental river-flow series goes back to 1954 for the Churchill River (Government of Canada 2018a). Analyses of trends and variability in regional streamflow in the

152 Northern Québec Labrador region show increase from 1970
 153 to 1979, decrease from 1980 to 1989, and increase from
 154 1990 to 2007 of annual and summer streamflow (Déry et al.
 155 2009; Jandhyala et al. 2009; Sveinsson Oli et al. 2008). In
 156 this region, the May to June discharge is principally influ-
 157 enced by snow/ice melting, and spring precipitation leading
 158 to spring flood peak, while precipitation mainly influences
 159 the July–September discharge (Robichaud and Mullock
 160 2001). During summer, temperature and humidity also play
 161 an important role for regional discharge as they influence
 162 water evaporation. Until now, only one study attempted to
 163 extend instrumental hydrological series in the Québec-Lab-
 164 rador peninsula. This study combined tree-ring indicators
 165 (widths, densities and stable isotope ratios), to understand
 166 past long-term water supply variability for the La Grande
 167 hydro-power generation system (15,240 MW) located at
 168 about 700 km west from Churchill River (Nicault et al.
 169 2014). Therefore, the main objective of this research is to
 170 produce long dendroisotopic series to: (1) evaluate their
 171 potential as proxies for reconstructing regional hydroclim-
 172 atic conditions over the last two centuries in the lower
 173 Churchill River region, and (2) understand past natural vari-
 174 ations in this area.

175 2 Materials and methods

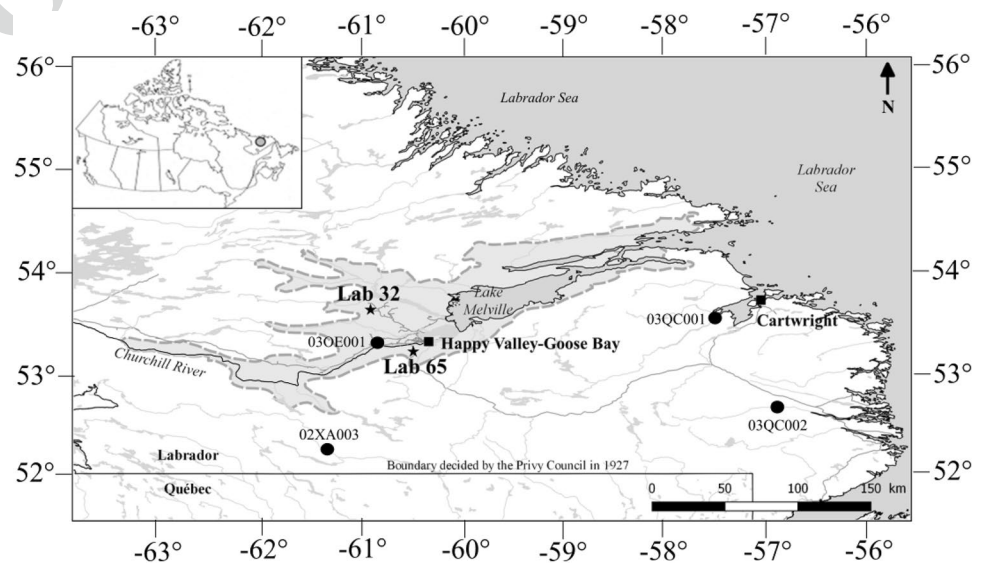
176 2.1 Study area and sample collection

177 The study area is located in the east-central part of
 178 Labrador, Canada (Fig. 1). The area sits on the eastern
 179 part of Precambrian Canadian shield formed during the
 180 Greenville orogeny. The bedrock is largely composed
 181 of quartzo-felspathic gneisses intruded by large body of

anorthosite-adamellite plutons emplaced during the Mid-
 dle Proterozoic (Greene 1974). The retreat of the Laurent-
 tide ice sheet during the last glaciation shaped the regional
 topography by leaving drumlins and rocky hills covered
 by a thin layer of ablation till. The valleys have been filled
 with Quaternary materials such as fluvio-glacial, fluvio-
 marine, fluvial or lacustrine sandy deposits (Dyke et al.
 2002; Payette et al. 1989). The study area is located in
 the High Boreal Forest ecoregion including Lake Melville
 and Churchill River valley. The relief is characterized by
 low altitude plateaus (≈ 500 m.a.s.l.) and river terraces
 remodelled by eolian activity. This ecoregion is part of
 the boreal forest biome with spruce-lichen forests on river
 terraces and on upland, and mixed forests on valley slopes
 (Government of Newfoundland Labrador 2018b).

The study area is part of the Interior Labrador climate
 zone defined as a continental regime with prevailing west-
 erly and southwesterly winds carrying relatively cool and
 dry air during long severe winters with deep snow cover,
 and warmer summer. However, the High Boreal Forest
 ecoregion experiences relatively shorter winters and cooler
 summers than surrounding ecoregions because of a biocli-
 matic gradient due to the converging effects of both mari-
 time and continental climatic influences (Nishimura and
 Laroque 2011; Roberts et al. 2006). The maritime climatic
 conditions are influenced by the cold Labrador Current
 bringing Arctic water along the Labrador coast (Sicre et al.
 2014; Trindade et al. 2011a). The Happy Valley-Goose
 Bay meteorological station registered from 1942 to 2009
 an average annual temperature of approximately 0.2°C
 and an average precipitation amounts of approximately
 1070 mm, 47% of which fall as snow (Government of
 Canada 2018b). The growth season lasted 130 days on
 average since 1942 with the average starting and ending

Fig. 1 Location of Lab 32 and Lab 65 sites (black stars) and hydrological stations (black circles) used for reconstruction and validation in the lower Churchill River region, Labrador. Weather station (Goose A) is located at Happy Valley-Goose Bay. The light grey zone represents the High Boreal Forest ecoregion



216 dates around the third week of May and second of October,
217 respectively (Government of Canada 2018c).

218 For the purpose of this research, two sites were selected
219 near the mouth of the Churchill River and Melville lake. Site
220 Lab 32 is located 50 km northwest of Happy Valley-Goose
221 Bay and 47 km north of the Churchill River (53°36'35.64"N,
222 60°53'07.08"W; Fig. 1). This site is at an altitude of
223 215 m.a.s.l., on a gentle slope of well-drained podzol, and is
224 covered by an old closed black spruce stand with lichens and
225 feather mosses. The till cover is discontinued by the pres-
226 ence of outcrops causing relatively heterogeneous edaphic
227 conditions. A total of 32 healthy (i.e., no visual health issues,
228 no wound or anomaly, straight growth), dominant or co-
229 dominant (i.e., representing well the group, growing under
230 low competition) black spruce [*Picea mariana* (Mill.) BSP]
231 specimens, aged from 50 to 290 years, were selected dur-
232 ing summer 2009 and fall 2010 for dendrochronological
233 analysis. Site Lab 65 is located 8 km south of the Churchill
234 River (53°11'50"N, 60°27'47"W; Fig. 1) at an altitude of
235 90 m.a.s.l.. The study site is an even-aged black spruce forest
236 growing on a well-drained brunisol. Twenty healthy black
237 spruce trees from this site were selected for dendrochron-
238 ological analysis during fall 2010.

239 For each tree, four cores were extracted with a 90° inter-
240 val at the standard height of 1.4 m with an increment borer
241 to establish the tree-ring chronologies (mean age of 185 and
242 193 years for sites Lab 32 and Lab 65, respectively). Each
243 core was subsequently sanded until wood cells were visible.
244 Tree rings were dated and measured with standard dendro-
245 chronological methods. A special care has been taken dur-
246 ing growth depression associated to outbreak events caused
247 by the presence of eastern spruce budworm [*Choristoneura*
248 *fumiferana* (Clem.); Boulanger and Arseneault 2004; Dobs-
249 berger et al. 1983; Nishimura 2009; Raske et al. 1986]. Dur-
250 ing the twentieth century, the most severe growth depres-
251 sions have been identified for the 1910–1920s, 1940–1950s,
252 1970–1980s periods over the Québec-Labrador peninsula.
253 A statistical analysis was then performed to confirm dat-
254 ing with the COFECHA program (Holmes 1983). For den-
255 droisotopic analysis, cross-section were sampled at breast
256 height on 5 and 4 specimens (minimum age of 100 years
257 and healthy appearance) among trees sampled at sites Lab
258 32 and Lab 65, respectively.

259 2.2 Sample preparation, treatment and isotopic 260 analysis

261 2.2.1 Inter-tree variabilities of isotope series

262 Prior to reconstructing dendroclimate, it is essential to estab-
263 lish the level of replication required and use an adapted pro-
264 tocol to yield a representative site signal with a satisfactory
265 signal-to-noise ratio. Although some researchers propose

266 averaging the isotope series from individual trees to produce
267 a single isotope series and characterize uncertainties related
268 to dendroclimatic reconstruction (Dorado Liñán et al. 2011;
269 McCarroll and Loader 2004), a realistic and more practical
270 approach would use pooling strategy on individual trees
271 prior to isolation of α -cellulose. This method yields similar
272 results to those obtained from averaging individual isotope
273 series whilst leading to a large reduction of sample numbers
274 that have to be prepared (Borella et al. 1998; Daux et al.
275 2018; Liu et al. 2015; Szymczak et al. 2012; Treydte et al.
276 2001; Woodley et al. 2012). Moreover, whereas four to five
277 trees were considered to be satisfactory to provide a repre-
278 sentative site scale signal, recent studies have demonstrated
279 that higher levels of replication (≥ 10 trees) based on confi-
280 dence intervals should be considered to obtain a more reli-
281 able low-frequency signal (Daux et al. 2018; Loader et al.
282 2013b). In addition, former studies have shown that varia-
283 tions within a ring are between 0.5–1.5‰, and 0.5–2.0‰
284 for $\delta^{13}\text{C}$ and $\delta^{18}\text{O}$ values, respectively (Leavitt 2010). There-
285 fore, in the present study, several cores per tree were selected
286 to overcome the intra-tree variability which can parasitize
287 the isotopic signal. In order to validate this approach and to
288 evaluate the inter-tree isotopic ranges, a test was performed.
289 Nine individual specimens were selected at both sites and
290 four radii were sub-sampled with a 90° interval from the
291 cross-section. In addition, previous research work at site
292 Lab 32 showed that it is relevant to use whole ring isotopic
293 signals instead of latewood values as there is no significant
294 difference between $\delta^{13}\text{C}$ and $\delta^{18}\text{O}$ values of latewood and
295 whole ring (Alvarez et al. 2018). Therefore, total wood from
296 annual tree rings were manually separated for 1960–1984
297 period using thin stainless-steel blades. After test validation,
298 the pooling method was applied to the rest of the chrono-
299 logical series. Same-year rings were combined by ensuring
300 that each tree has the same mass contribution with 1-year
301 resolution at site Lab 65, and with 2-year and 1-year resolu-
302 tion for 1800–1939 and 1940–2009 periods, respectively, at
303 site Lab 32.

2.2.2 Extraction of α -cellulose and isotopic analysis

304 Samples were homogenized in a Wiley grinding 40 mesh
305 mill and then placed in tightly sealed fiber filter bags
306 (Ankom F57) for subsequent chemical treatments. The
307 α -cellulose from all samples was extracted as it contains
308 the strongest environmental signal compared with bulk wood
309 for boreal black spruce trees (Bégin et al. 2015). Briefly, the
310 protocol consisted in removing organic soluble compounds
311 using consecutive mixture of benzene/methanol (1:1),
312 acetone and demineralized water. Afterward, lignin was
313 removed using a solution of demineralized water, sodium
314 chlorite and pure glacial acetic acid. Holocellulose was sep-
315 arated using a 17% sodium hydroxide solution. The remaining
316

317 α -cellulose in fiber filter bags was then soaked in a 10% acetic acid solution, carefully rinsed with demineralized water and dried overnight.

320 The $\delta^{13}\text{C}$ and $\delta^{18}\text{O}$ values were measured on a total of 321 1790 samples at the Delta-Lab of the Geological Survey of Canada, in Québec City. All cellulose samples were analyzed using an elemental analyzer (Costech) for $\delta^{13}\text{C}$ and a thermal conversion elemental analyzer (TC/EA; Finnigan Mat) for $\delta^{18}\text{O}$ measurements, coupled to an isotope ratio mass spectrometry (Delta Plus XL; Finnigan Mat). The isotopic ratios are reported with the conventional δ notation relative to VPDB for carbon isotopes and VSMOW for oxygen isotopes in permil (‰). The analytical accuracies of these instruments were 0.1‰ for $\delta^{13}\text{C}$ and 0.2‰ for $\delta^{18}\text{O}$, and established using international and in-house standards (NBS-19, LSVEC, IAEA-CH-6 and vanillin for $\delta^{13}\text{C}$ and IAEA-602, IAEA-C3, vanillin and sucrose for $\delta^{18}\text{O}$). The external analytical precision obtained from 180 replicates were 0.1 and 0.2‰ for $\delta^{13}\text{C}$ and $\delta^{18}\text{O}$ values, respectively. Complete $\delta^{13}\text{C}$ series were corrected to account for anthropogenic changes in the atmospheric CO_2 $\delta^{13}\text{C}$ values (data used from McCarroll and Loader 2004 and the Scripps CO_2 program) and increase of atmospheric concentration (pCO_2). To correct for the latter on plant response, we converted the Matlab code from McCarroll et al. (2009) to the R code that follows a 6-steps procedure (see Supplementary material). This correction mainly attempts to obtain $\delta^{13}\text{C}$ values close to what they could have been under pre-industrial conditions by assuming a passive response to rising pCO_2 and applying a loess regression to extract $\delta^{13}\text{C}$ low-frequency changes.

347 2.3 Hydroclimatic data and statistical approach

348 In order to reconstruct regional discharge in the lower Churchill River region, we evaluated (1) the influence of climatic conditions on tree-ring isotope series and regional discharge, and (2) the relationship between tree-ring isotope series and regional discharge. To this aim all statistical analyses and reconstruction were performed using the R software (Core Team 2018).

355 2.3.1 Climatic and hydrologic series

356 The Adjusted and Homogenized Canadian Climate Data (AHCCD) from the Goose Bay weather station, located at the Canadian Forces Base of Goose Bay, were used (Goose A station data available at <http://ec.gc.ca/dccha-ahccd>). Complete and continuous total precipitation and temperature series have been recorded at the station since 1942. The investigated climatic series included total monthly precipitations (P_{total}), monthly maximum, minimum and average temperatures (T_{max} , T_{min} and T_{mean} , respectively), and vapor pressure deficit (VPD) integrating temperature and

relative humidity (Allen et al. 1990) for a 15-month period (from July of the previous growing season until September of the current year).

The Churchill River gauge station (Fig. 1; 03OE001) record was disrupted after impoundment of the river for the production of hydroelectric power in 1971 by Hydro-Québec and Churchill Falls (Labrador) Corporation (Grimard and Jones 1982). Natural discharge data are therefore only available for the 1954–1971 period, which is insufficient to calibrate the model and produce a robust reconstruction. In order to extend instrumental data series and produce a regional discharge index, the discharge series of three rivers close to the Churchill river were normalized by dividing each year-value by the average of the series for the common 1979–2009 period, which corresponds to the period covered by the shortest series (River_{index}; Fig. 1; 03QC001, Eagle River, 1969–2009; 03QC002, Alexis River, 1978–2009; 02XA003, Little Mecatina River, 1979–2009; Government of Canada 2018a). The resulting normalized river series were then averaged for each year on a 15-month period (same as climatic series).

2.3.2 Relationships between tree-ring isotope series and regional discharge

To obtain the same temporal resolution between the two sites, the Lab 32 series were annualized using a cubic spline interpolation for 1800–1939 period. The $\delta^{13}\text{C}$ and $\delta^{18}\text{O}$ series were averaged between sites to obtain a unique carbon and oxygen series ($\delta^{13}\text{C}_{\text{mean}}$ and $\delta^{18}\text{O}_{\text{mean}}$) for understanding tree processes and their relationship with climatic conditions. Under boreal environments, climatic variables, which are linked to one another, concur in influencing $\delta^{13}\text{C}$ and $\delta^{18}\text{O}$ values. For that reason, the $\delta^{13}\text{C}$ and $\delta^{18}\text{O}$ series covary and they can be combined to obtain a unique isotopic series integrating a multi-variable regional signal. In other words, the combination of both isotopes provides complementary climatic information (Ferrio and Voltas 2005). As the variable aimed to be reconstruct (discharge) integrates the influence of different climatic variables, which also influence tree-ring isotope series, the isotopic series have to be combine to integrate maximum of information. This approach also minimizes the non-climatic portion of the isotopic signals which increases statistical relationship with hydroclimatic variables (Bégin et al. 2015; Loader et al. 2008; McCarroll et al. 2003). The $\delta^{13}\text{C}$ and $\delta^{18}\text{O}$ series from the two sites were thus combined with a z-score ($\delta^{13}\text{C}_{\text{combined}}$ and $\delta^{18}\text{O}_{\text{combined}}$) in order to give a similar weight at each isotopic ratio for reconstruction purpose. This method was supported by the weighted approach proposed by McCarroll et al. (2003) which is based on the percentage of total variation explained by each isotope. Using this weighted approach,

417 the $\delta^{13}\text{C}$ and $\delta^{18}\text{O}$ accounted for 51 and 49% of the river
 418 discharge variations, respectively. Pearson correlation
 419 coefficients were then calculated to examine the statisti-
 420 cal relationships between tree-ring isotope series, climatic
 421 variables/derived parameter and regional discharge series.
 422 A linear simple regression model was used to fit the rela-
 423 tionship between the combined tree-ring isotopic series
 424 ($\delta^{13}\text{C}_{\text{combined}}$) and regional discharge series (average
 425 June, July and August River_{index}), and summer River_{index}
 426 was then reconstructed back to 1800. Therefore, the dis-
 427 charge reconstruction was based on nine trees from two
 428 sites located at ca. 50 km from each other. In order to
 429 assess the robustness of the calibration model, a twofold
 430 cross-validation technique was used on instrumental data
 431 (covered period: 1969–2009). Root mean squared error
 432 (RMSE) and coefficient of determination (R^2) were cal-
 433 culated for calibration period, while Reduction of Error
 434 (RE) and Coefficient of Efficiency (CE) were calculated to
 435 evaluate reconstruction skills (Briffa et al. 1988).

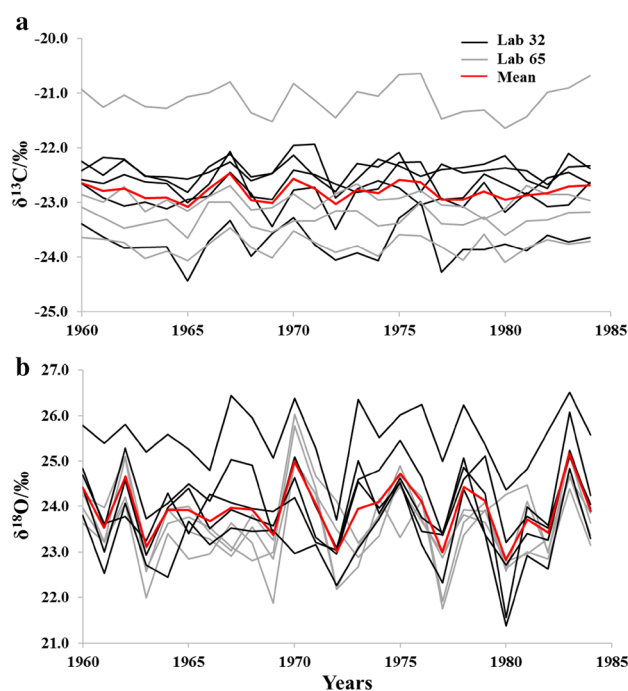
436 2.3.3 Reconstruction validation

437 In the perspective of reconstruction validation, independ-
 438 ent reconstructions are essentials. However, neither long
 439 instrumental streamflow records, nor reconstruction based
 440 on independent proxies or methods to compare with tree-
 441 ring isotope reconstruction did exist prior to this study
 442 in the investigated region. Streamflow variability recon-
 443 struction from tree-ring series and ANATEM model have
 444 been tested and compared over the 1881–2011 period in
 445 northern Québec. The results obtained suggested that dif-
 446 ferent reconstruction methods have to be applied within
 447 the same catchment for the purpose of comparison and
 448 validation (Brigode et al. 2016). Hence, the ANATEM
 449 reconstruction model was applied. ANATEM offers the
 450 advantage of combining local observations and large-scale
 451 climatic information such as geopotential heights field to
 452 reconstruct a past climatic ensemble (temperature and pre-
 453 cipitation) based on synoptic situation similarities between
 454 days from recent and past periods. Then, a rainfall–run-
 455 off model—previously calibrated on the observed period
 456 using available discharge series—is used to transform this
 457 climatic series into streamflow series (for more details see
 458 Brigode et al. 2016; Kuentz et al. 2015). Therefore, the
 459 model was applied for the 1880–2009 period using the
 460 following hydroclimatic: geopotential heights from NOAA
 461 20CR reanalysis (Compo et al. 2011), air temperature from
 462 the Berkeley Earth Surface Temperature (Rohde et al.
 463 2014), air temperature and precipitation from the NRCan
 464 gridded dataset (Hutchinson et al. 2009) and discharge
 465 data from the three individual rivers (Eagle River, Alexis
 466 River and Little Mecatina River).

467 3 Results

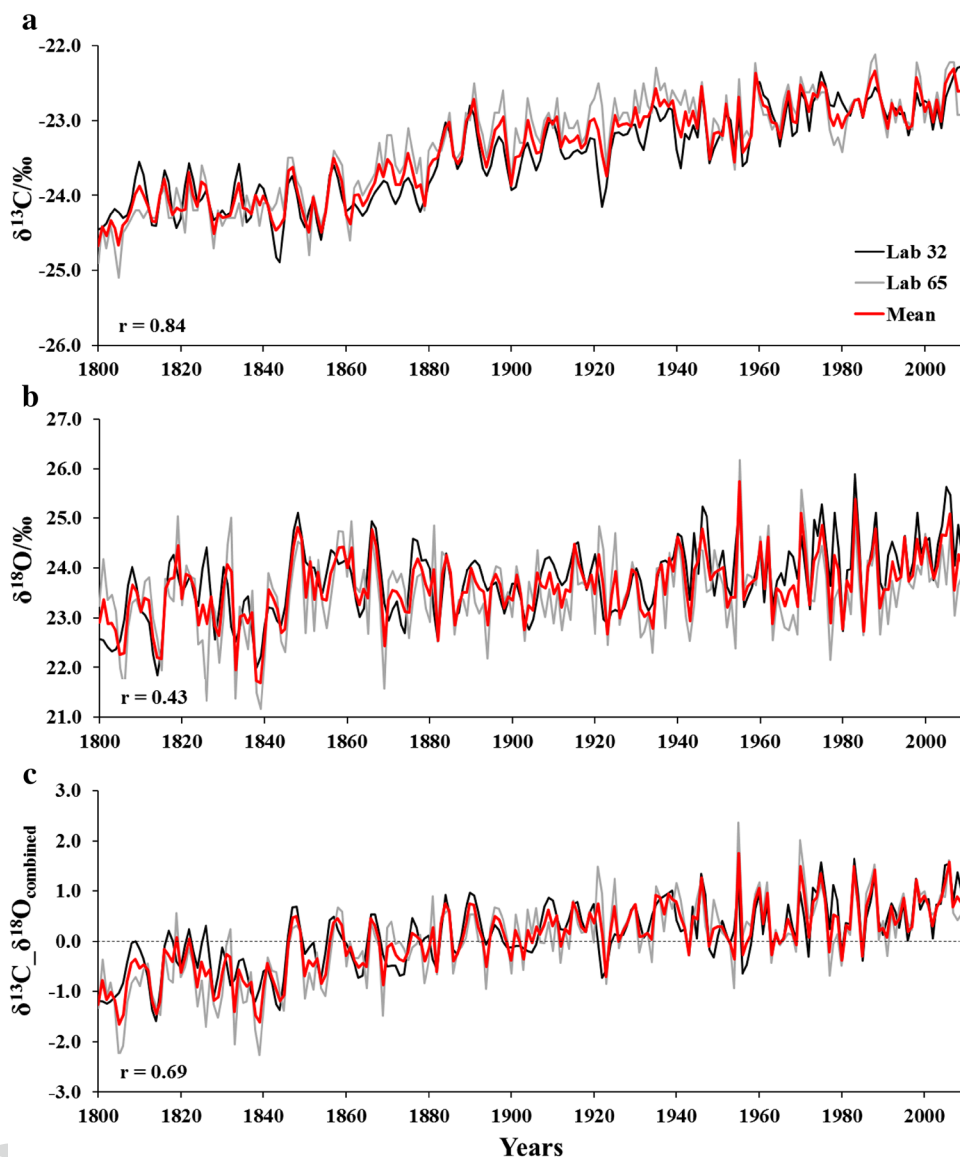
468 3.1 Inter-tree variabilities of isotope series

469 At the studied sites, the $\delta^{13}\text{C}$ values of the nine individual
 470 trees varied from -24.4 to -20.6‰ (Fig. 2a) after correc-
 471 tion for the Suess effect and increase of pCO_2 , and de-trend-
 472 ing of the series with a high-pass filter. Eight of the trees,
 473 within the same range of absolute values, show an aver-
 474 age of -23.0‰ , whereas one tree has a higher average at
 475 -21.1‰ . For the $\delta^{18}\text{O}$ values (Fig. 2b), all trees are within
 476 the same range with values from 21.4 to 26.1‰ and an aver-
 477 age of 23.7‰, excepted one which has an average of 25.5‰.
 478 Moreover, ring width series decrease from 1910 to 1920,
 479 1950 to 1957 and 1974 to 1981, with minimal growth associ-
 480 ated with outbreak episodes in 1915, 1952 and 1977, respec-
 481 tively (Fig. S2). During the 1910–1920 and 1950–1957 epi-
 482 sode, $\delta^{13}\text{C}$ and $\delta^{18}\text{O}$ values are relatively constant (Fig. 3a,
 483 b, respectively) suggesting no specific influence from bud-
 484 worm defoliation on isotopic signals. During the 1974–1981
 485 episode, $\delta^{13}\text{C}$ mean values decrease from 1975 to 1978 and
 486 increase from 1979 to 1984 (Fig. 2a). Those observations
 487 are opposite to those of previously studied black spruce
 488 trees (Simard et al. 2008, 2012). The $\delta^{18}\text{O}$ mean values
 489 show two decreases in 1977 and 1980 for almost each trees



489 **Fig. 2** Tree-ring $\delta^{13}\text{C}$ corrected and de-trended (**a**) and $\delta^{18}\text{O}$ de-
 490 tided values (**b**) for the nine individual trees from site Lab 32
 491 (black line) and Lab 65 (grey line). Red line is the mean of the nine
 492 trees

Fig. 3 Tree-ring $\delta^{13}\text{C}$ series at sites Lab 32 (black line) and Lab 65 (grey line), and regional $\delta^{13}\text{C}_{\text{mean}}$ (red line) (a); tree-ring $\delta^{18}\text{O}$ series (b); and the resulting final isotopic series combined using z-score (c), see 2.3 for details



490 (Fig. 2b). Such decreases are also observed during other
 491 years not related to budworm outbreak episodes. One explanation
 492 could be that black spruce is a tertiary food source for
 493 budworm after balsam fir and white spruce likely yielding
 494 less severe tree defoliation during the outbreak episodes in
 495 Labrador (Nishimura 2009). This is particularly due to the
 496 speed of shoot development during spring. Balsam fir and
 497 white spruce shoots develop faster, which makes them more
 498 susceptible to defoliation (Blais 1962; Nealis and Régnière
 499 2004). In all likelihood, tree-ring $\delta^{13}\text{C}$ and $\delta^{18}\text{O}$ series at Lab
 500 32 and Lab 65 are not significantly influenced by budworm
 501 defoliation during outbreak episode. Even through two trees
 502 show higher values for $\delta^{13}\text{C}$ and $\delta^{18}\text{O}$ series likely related
 503 to metabolic differences or edaphic conditions, inter-tree $\delta^{13}\text{C}$
 504 and $\delta^{18}\text{O}$ values from the nine selected trees show signifi-
 505 cant statistical correlation ($r=0.40$ and 0.59 , respectively),
 506 resulting in a high expressed population signal (EPS; 0.86

and 0.93 for $\delta^{13}\text{C}$ and $\delta^{18}\text{O}$, respectively). The EPS values
 for $\delta^{13}\text{C}$ is slightly higher than the acceptable threshold of
 0.85 , while it is higher for the $\delta^{18}\text{O}$ (Buras 2017; Wigley
 et al. 1984) meaning that for this study, nine trees are suffi-
 cient to represent the site signal, which allows pooling tree
 ring from same years and obtaining $\delta^{13}\text{C}$ and $\delta^{18}\text{O}$ series
 for sites Lab 32 and Lab 65. Those results are in accordance
 with the number of trees suggested by Daux et al. (2018;
 8 and 10 trees for $\delta^{13}\text{C}$ and $\delta^{18}\text{O}$, respectively) to generate
 an isotopic mean series representative of the population for
 conifer species.

3.2 Tree-ring $\delta^{13}\text{C}$ and $\delta^{18}\text{O}$ series at the two studied sites

In the studied area, tree-ring corrected $\delta^{13}\text{C}$ values of the
 two selected sites (not de-trend) are significantly correlated

($r=0.84$; $p<0.05$; $n=210$; Fig. 3a). The long-term trend of the $\delta^{13}\text{C}_{\text{mean}}$ (mean for Lab 32 and Lab 65 sites) fluctuates around -24.1% from 1800 to 1859 followed by an increase between 1860 and 1959 and fluctuates around -22.8% between 1960 and 2009. The $\delta^{13}\text{C}_{\text{mean}}$ inter-annual variations fluctuate between -24.8 and -22.3% with an average of -23.4% . There is also a statistically significant correlation between $\delta^{18}\text{O}$ isotopic series of Lab 32 and Lab 65 ($r=0.43$; $p<0.05$; $n=210$; Fig. 3b). The $\delta^{18}\text{O}_{\text{mean}}$ of the two sites shows a steady increase from 1800 (22.9%) to 2009 (24.0%), short-term variations between 21.6 and 25.7%, and an average value of 23.6%.

The individual $\delta^{13}\text{C}_{\text{mean}}$ and $\delta^{18}\text{O}_{\text{mean}}$ series show significant complementarity ($r=0.45$; $p<0.05$; $n=210$) as they are highly, but differently, correlated with the same climatic variable/derived parameter (T_{max} and VPD; Table 1). The $\delta^{13}\text{C}_{\text{mean}}$ and $\delta^{18}\text{O}_{\text{mean}}$ series of Lab 32 and Lab 65 are thus highly correlated ($r=0.69$; $p<0.05$; $n=210$; Fig. 3c), allowing their combination to obtain a single isotopic series representative of the lower Churchill River region hydroclimatic conditions. The $\delta^{13}\text{C}_{\text{mean}}$ and $\delta^{18}\text{O}_{\text{mean}}$ series for the two sites shows a flat trend from 1800 to 1849 followed by an increase between 1850 and 1959 and a flat trend between 1960 and 2009.

3.3 Relationships between isotopic series and hydroclimatic variables

The $\delta^{13}\text{C}_{\text{mean}}$ and $\delta^{18}\text{O}_{\text{mean}}$ series display significant correlations with some climatic variables (Table 1). The regional $\delta^{13}\text{C}_{\text{mean}}$ shows the highest correlation with T_{max} and VPD from May–August. Oxygen isotopic ratios have an inverse correlation with P_{total} and a positive correlation with VPD and T_{max} for the same period. Therefore, the final $\delta^{13}\text{C}_{\text{mean}}$ and $\delta^{18}\text{O}_{\text{mean}}$ series correlates well with the three climatic variables. There are also inverse statistically significant correlations between the $\delta^{13}\text{C}$ and $\delta^{18}\text{O}_{\text{mean}}$ and $\text{River}_{\text{index}}$ from

Table 1 Significant statistical correlations between the tree-ring isotopic series and hydroclimatic variables (all correlations are significant at $p<0.05$, $n=41$)

	T_{max}	P_{total}	VPD	$\text{River}_{\text{index}}$
$\delta^{13}\text{C}_{\text{mean}}$	0.64 ^a	-0.36 ^a	0.65 ^a	-0.60 ^d
$\delta^{18}\text{O}_{\text{mean}}$	0.53 ^a	-0.42 ^a	0.56 ^a	-0.58 ^d
$\delta^{13}\text{C}_{\text{mean}}-\delta^{18}\text{O}_{\text{mean}}$	0.63 ^a	-0.45 ^a	0.66 ^a	-0.66 ^d
$\text{River}_{\text{index}}$	-0.49 ^b	0.63 ^c	-0.60 ^e	-

Selected bold periods are for both variables

^aMay–August

^bJune to Sept

^cMay to Sept

^dJune–August

^eMay–August VPD correlated with June–August $\text{River}_{\text{index}}$

June–August and the highest correlations are found for the final $\delta^{13}\text{C}_{\text{mean}}-\delta^{18}\text{O}_{\text{mean}}$ series ($r=-0.56$, -0.55 , -0.31 , -0.66 for June, July, August and average June–August $\text{River}_{\text{index}}$, respectively; $p<0.05$; $n=41$). The relationships between $\text{River}_{\text{index}}$ and climatic factors suggest that spring end and summer conditions are important drivers on regional discharge.

3.4 Regional discharge reconstruction from the tree-ring $\delta^{13}\text{C}$ and $\delta^{18}\text{O}$ combination

The summer regional discharge (June–August) in the lower Churchill River region was reconstructed for the 1800–2009 period (Fig. 4). The quality of reconstruction is assessed based on a cross-validation method (Table 2). The R^2 of the two calibrated periods are highly significant ($p<0.01$) and both RE and CE of the verification periods are >0 which indicates that the model skills are adequate (Cook et al. 1999). The R^2 of the total period ($R^2=0.44$; used for the final reconstruction) shows excellent coherence between observations and simulations of the $\text{River}_{\text{index}}$. The significant statistical correlation between discharge index reconstruction and natural discharge data from the lower Churchill River ($R^2=0.31$; $p<0.05$; $n=18$) validates the predictive ability of the model. Moreover, reconstructed June–August discharge series show varying climatic conditions over the last 200 years with a long-term decrease from 1800 to 2009 and short-term decreases that are associated to drought periods (e.g., 1935–1954, 1982–1990) when compared with the drought index of Standardized Precipitation-Evapotranspiration Index (SPEI03; Begueria et al. 2018).

3.5 Isotopic reconstruction compared with the ANATEM reconstruction

Overall, the ANATEM method results show a good fit with the tree-ring isotope series reconstruction, with a statistically significant correlation ($r=0.41$; $p<0.05$; $n=130$; Fig. 5). The two reconstructions show a long-term decrease of summer discharge, all along the studied period. Moreover, the reconstructed interannual variabilities are quite similar for the 1941–2009 period, while they are different between 1880 and 1940. One explanation could be that trees from the study region are barely sensitive to precipitation variability as water availability is not a limiting factor due to the annual high supply in precipitation (around 1070 mm/year from 1942 to 2009). Thus, short term variations of discharge reconstructed from tree-ring isotopic series might not respond readily to the precipitation variability, whereas the ANATEM discharge reconstruction uses precipitation variability as an input variable. Another explanation could be related to the climatic reanalysis used by the ANATEM model. Scarce geopotential height data before 1950 (Cram et al. 2015) might increase error on

Fig. 4 Summer regional discharge (June–August; **a**) reconstructed from the combined tree-ring isotopic series ($\delta^{13}\text{C}$ – $\delta^{18}\text{O}$ combined) for the 1800–2009 period (black line), with 5-year moving average (red line). Error bars represent the 95% confidence interval. The modeled reconstruction is also compared with the observed River_{index} for the 1969–2009 period (solid grey line; upper right scatterplot), the observed Churchill River discharge for the 1954–1971 period (03OE001 station; open grey line; upper central scatterplot) and the summer SPEI 3-month

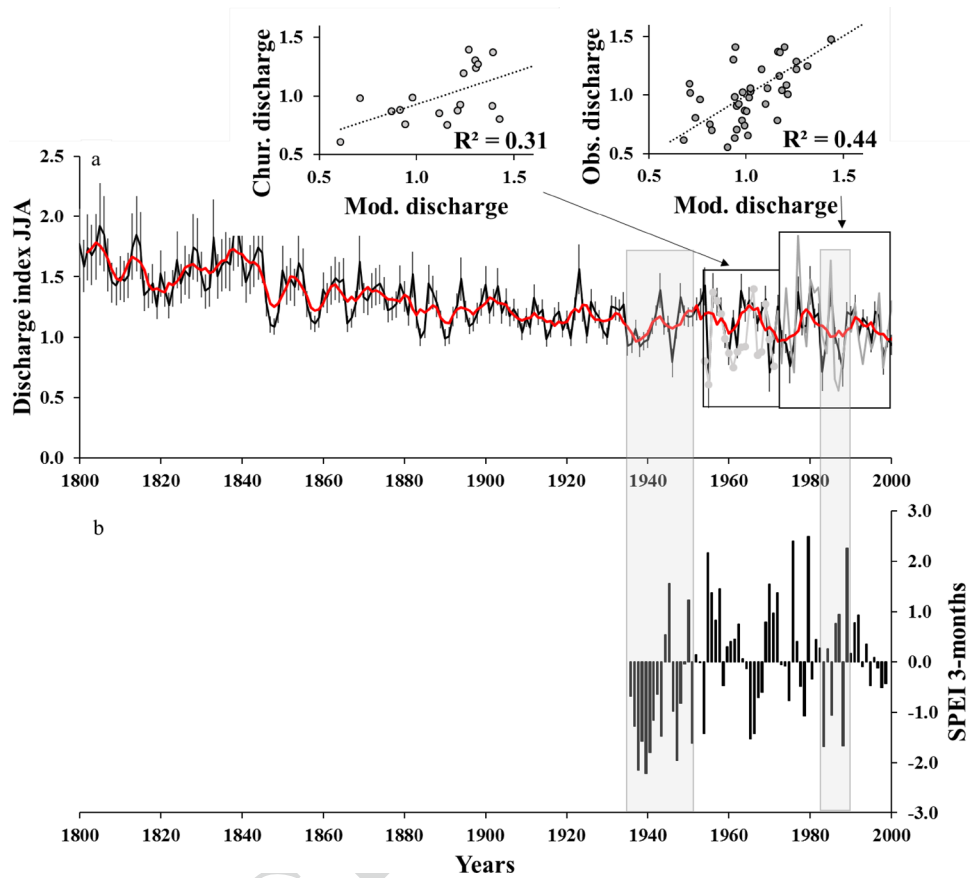


Table 2 Statistics of model calibrations using a simple linear regression method

	Calib 1969– 1988	Verif 1989– 2009	Calib 1989– 2009	Verif 1969– 1988	Total period 1969–2009
R ²	0.45		0.43		0.44
RMSE	0.24	0.20	0.16	0.27	0.22
RE		0.42		0.44	
CE		0.13		0.32	

Coefficient of determination (R²) and root mean square error (RMSE) are given for calibration steps while reduction of error (RE) and coefficient of efficiency (CE) are given for the verification steps

605 precipitation reconstruction used for the rainfall-runoff model
606 and thus on discharge reconstruction in the region.

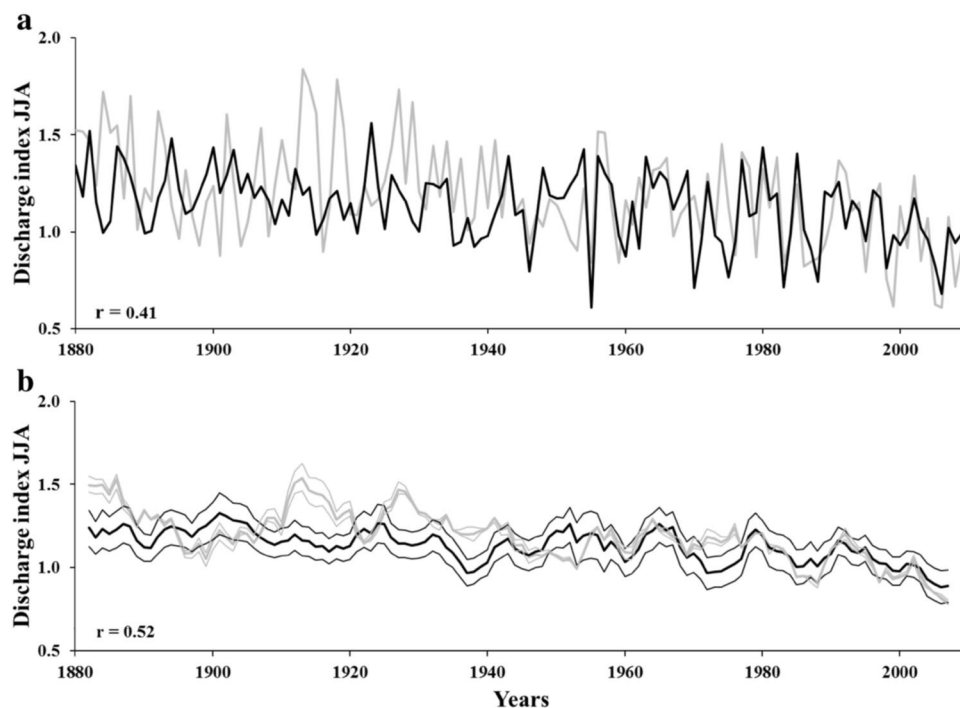
607 4 Discussion

608 4.1 Relationships between climatic conditions, 609 tree-ring stable isotopes and regional discharge

610 Streamflow reconstruction from tree-ring $\delta^{13}\text{C}$ and $\delta^{18}\text{O}$ val-
611 ues entails understanding the existing relationships between

612 climatic conditions, tree-ring isotopes and water resource. 612
613 Although the effect of climatic variables is relatively direct 613
614 on processes controlling isotopic fractionation and water 614
615 variability, the relationships between river flow and tree- 615
616 ring isotopes are indirect. Two isotope-based river-flow 616
617 reconstructions from tree rings invoked key mechanisms 617
618 to explain the cause and effects links between $\delta^{13}\text{C}$ series 618
619 and river flows (Waterhouse et al. 2000; Wils et al. 2010). 619
620 In the present study, Lab 32 and Lab 65 are located at 47 620
621 and 8 km, respectively, from the Churchill River, which dis- 621
622 cards the direct influence of river moisture to trees invoked 622
623 by Waterhouse et al. (2000). Moreover, under the known 623
624 climatic conditions of the region, water availability is not a 624
625 limiting factor for tree growth and could rather be a reducing 625
626 factor for climate sensitivity of tree-ring width chronologies 626
627 (Nishimura and Laroque 2011; Trindade et al. 2011b). At 627
628 Lab 32 and 65, tree-ring width series show inconsistent or 628
629 non-significant correlations with climatic variables (data not 629
630 show), while tree-ring isotope series significantly correlate 630
631 with summer conditions. Those climatic conditions directly 631
632 influence stomatal aperture of tree needles, photosynthesis 632
633 and the distillation of cloud masses that regulate tree-ring 633
634 $\delta^{13}\text{C}$ and $\delta^{18}\text{O}$ variations. Using tree-ring stable isotopes 634
635 rather than width is thus recommended for reconstructing 635
636 river discharge in the climatic context of this study. 636

Fig. 5 Summer discharge reconstruction using tree-ring isotopes (black line) and the ANATEM method (grey line) for **a** raw yearly data, and **b** 5-year moving average data with 95% confidence interval



637 The weak correlation between tree-ring $\delta^{13}\text{C}$ values and
 638 precipitation suggests that precipitation is not the main
 639 control on carbon fractionation in trees of the area. This
 640 interpretation makes sense as the abundance of precipita-
 641 tion provides unlimited water supplies to the trees (Bégin
 642 et al. 2015; Naulier et al. 2015b; Porter et al. 2009; Saurer
 643 et al. 2004). In addition, in this non water-limited context,
 644 the photosynthetic capacity is mainly influenced by temper-
 645 ature and sunshine conditions, and exerts the principal
 646 control on carbon assimilation (Gagen et al. 2011; Loader
 647 et al. 2013a). The significant correlation between $\delta^{13}\text{C}_{\text{mean}}$
 648 and T_{max} from May to August supports this interpretation.
 649 To a lesser extent, there is a potential control of relative
 650 humidity on ^{13}C fractionation via stomatal conductance as
 651 $\delta^{13}\text{C}_{\text{mean}}$ values correlate with May–August VPD (Schei-
 652 degger et al. 2000).

653 Relationships found between tree-ring $\delta^{18}\text{O}_{\text{mean}}$ and
 654 May–August T_{max} , P_{total} and VPD indicate that these climatic
 655 variables and derived parameters are the main controls on
 656 the oxygen isotopic fractionation, which is consistent with
 657 the following well-known mechanisms. Temperature con-
 658 trols the precipitation amount, type (rain, snow, etc.) and
 659 isotopic fractionation during droplet formation from clouds
 660 (Clark and Fritz 1997; Dansgaard 1964), while a combina-
 661 tion of temperature, precipitation and humidity affects sto-
 662 matal functioning (Saurer et al. 1997). The VPD positive
 663 correlation with the $\delta^{18}\text{O}_{\text{mean}}$ values confirms the influence
 664 of those climatic variables on plant transpiration, and thus,
 665 on the ^{18}O discrimination occurring at the leaf level (Ferrio
 666 and Voltas 2005).

667 At a broader scale, a site located 660 km west in Que-
 668 bec from Lab 32 and Lab 65, shows tree-ring $\delta^{18}\text{O}$ average
 669 around 3‰ lighter (Naulier et al. 2014) than the signal at
 670 the presently studied sites. In this area, climate is continen-
 671 tal and subarctic with short, mild summers and long, cold win-
 672 ters with a dominance of arctic winds under the influence of
 673 Labrador Current. These results suggest a continental effect
 674 of the water $\delta^{18}\text{O}$ fractionation when clouds move inland
 675 from the open Labrador Sea. Moreover, in the study region,
 676 a bioclimatic gradient has been observed through the rela-
 677 tionship between tree-ring width and summer temperature
 678 (Nishimura and Laroque 2011): the most eastern sites show
 679 a significant relationship between tree growth and July tem-
 680 peratures, whereas the western sites tended to correlate with
 681 May, June and August temperatures. The authors interpreted
 682 these results as demonstrating a bioclimatic gradient from
 683 coastally proximal, maritime-influenced sites, and inland,
 684 continentally influenced sites, with transition occurring
 685 approximately 330 km inland from the coast. The $\delta^{13}\text{C}_{\text{mean}}$
 686 and $\delta^{18}\text{O}_{\text{mean}}$ values of the lower Churchill River region at
 687 about 230 km from the coast are thus most likely influenced
 688 by maritime climate impacted by the cold Labrador Cur-
 689 rent. Finally, other studies have demonstrated similar corre-
 690 lations between temperature, precipitation, VPD, and black
 691 spruce isotope series in cold environment (Bégin et al. 2015;
 692 Naulier et al. 2014). These studies along with the present one
 693 thus show that black spruce trees are sensitive to the same
 694 climatic variables within the Québec-Labrador peninsula.

695 Results also show significant correlations between June to
 696 September River_{index} and T_{max} , May to September River_{index}

697 and P_{total} , and June–August River_{index} and May–August VPD.
 698 They strongly suggest that the climatic variables controlling
 699 tree-ring stable isotopes are also the main drivers influencing
 700 regional discharge during summer. This observation agrees
 701 with few others studies showing that both water supply and
 702 tree-ring indicators are controlled by similar combinations of
 703 climatic variables in the Canadian northeastern boreal forest
 704 (Bégin et al. 2015; Nicault et al. 2014). These mechanisms
 705 explain the significant inverse correlation found between
 706 $\delta^{13}\text{C}_{\text{mean}}$ and $\delta^{18}\text{O}_{\text{mean}}$ with River_{index} from June to August.
 707 The combination of T_{max} , VPD and P_{total} triggers this indirect
 708 relationship, each at various degrees. In practical terms, dur-
 709 ing wet and cold summer conditions, low T_{max} , VPD and high
 710 P_{total} decrease tree-ring $\delta^{13}\text{C}$ and $\delta^{18}\text{O}$ values and increase
 711 water discharge, and dry and hot summer conditions gener-
 712 ate the opposite. Moreover, terrestrial biosphere models
 713 have demonstrated that plant transpiration directly influences
 714 land surface water regimes during summer. Soil moisture and
 715 continental runoff decrease when stomatal opening releases
 716 water from trees, and they increase when stomatal closure
 717 retains water (Betts et al. 2007; Cao et al. 2010; Gedney et al.
 718 2006; Knauer et al. 2017). Throughout a study across Can-
 719 ada, Wang et al. (2013) have shown that evapotranspiration
 720 is mainly controlled by surface heat fluxes in regions where
 721 water is abundant. For the studied region, this means that
 722 temperature, sunshine and VPD partly influenced stomatal
 723 conductance, and then evapotranspiration, which directly
 724 influences summer regional discharge. All of these interpre-
 725 tations strengthen the postulate that the tree-ring $\delta^{13}\text{C}$ and
 726 $\delta^{18}\text{O}$ combination can serve to reconstruct summer regional
 727 discharge. Reconstruction from the ANATEM method sup-
 728 ports this point as it significantly correlates with the tree-ring
 729 isotopic reconstruction (Fig. 5). The two discharge recon-
 730 structions show a significant long-term decrease suggesting
 731 that this part of Canada has experienced an overall decrease
 732 in summer discharge over the past 200 years. This observa-
 733 tion is in accordance with studies showing evidences of high
 734 water level during the first half of the nineteenth century that
 735 has been recognized as one of the coldest intervals of the
 736 Little Ice Age with the persistence of cold and humid condi-
 737 tions in northern Québec (Bégin and Filion 1988; Bhiry et al.
 738 2011). In addition, when comparing the tree-ring isotopic
 739 reconstruction with discharge instrumental series located as
 740 far as 900 km north west and 1300 km south west (Grand
 741 Baleine and Harricana River, respectively), a similar decrease
 742 is observed since 1915 (Fig. S3). Those results suggest that
 743 likely all the Québec-Labrador peninsula experienced a gen-
 744 eral decrease in the summer river discharge. Interestingly,
 745 tree-ring stable isotopes series and consequently summer
 746 discharge reconstruction series show significant correlation
 747 with the AO that potentially influences the observed long-
 748 term discharge decrease (Thompson and Wallace 2000), and
 749 this relationship is dealt with in the next section.

4.2 Teleconnections between large-scale atmospheric variability and reconstructed discharge

750
751
752
753 Over various Canadian regions, large-scale atmospheric and
754 oceanic variability modes influence seasonal climate and
755 the stronger links are generally reported to occur during the
756 cold season, while less robust relationships are described for
757 summer (Bonsal and Shabbar 2008). Some studies also find
758 a significant lagged relationship between winter El Niño/
759 Southern Oscillation, Atlantic Multidecadal Oscillation,
760 Pacific North American, NAO and AO, and spring to sum-
761 mer climate (Asong et al. 2018; Ogi et al. 2003, 2004; Shab-
762 bar and Skinner 2004). Ogi et al. (2004) suggested that there
763 is a persistence from one mode of the NAO/AO in winter to
764 a similar mode in summer. In northern/northeastern Canada,
765 winter climatic conditions are mainly driven by winter NAO
766 and AO, which are strongly linked (both showing positive
767 phases driving anomalously cold temperatures during win-
768 ter; D'Arrigo et al. 2003; Rogers and McHugh 2002; Thomp-
769 son and Wallace 2001). The AO represents the atmospheric
770 mass exchange between middle and high latitudes and it is
771 frequently discussed along with the NAO as they resemble
772 in many aspects (Thompson and Wallace 1998). Changes in
773 atmospheric circulation associated with these oscillations
774 can thus lead to changes in seasonal climatic conditions.
775 Other studies have emphasized the important influence
776 of NAO/AO on tree growth and biomass production dur-
777 ing summer in the northeastern part of Canada (Boucher
778 et al. 2017; Buermann et al. 2003; Cho et al. 2014; Ols et al.
779 2018). Some of these studies discuss the impact of winter
780 atmospheric conditions associated with NAO/AO on spring
781 and summer tree activities. For example, a positive phase of
782 winter NAO/AO enhanced cooler and drier conditions and
783 decreases the normalized difference vegetation index during
784 the following spring. However, growth of black spruce trees
785 from Quebec responds to summer, rather than winter, NAO
786 and AO with a significant negative relationship since 1980
787 (Ols et al. 2018). Interestingly, in the present study, the final
788 $\delta^{13}\text{C}_{\text{mean}}\text{-}\delta^{18}\text{O}_{\text{combined}}$ series do not show statistical links with
789 the NAO, but is positively correlated with the summer AO
790 index ($r = 0.37$; $p < 0.05$; $n = 101$).

791 As tree-ring isotopic series and river discharge are
792 inversely correlated and respond to similar climatic con-
793 ditions, the summer discharge reconstruction necessarily
794 shows an inverse correlation with summer AO (Fig. 6).
795 Similar results have been observed by Nicault et al. (2014)
796 between reconstructed summer discharge and summer AO
797 index ($r = -0.42$; $p < 0.05$) at a site located 700 km west from
798 the Churchill River. These authors found low, but significant
799 correlations between the summer AO/NAO and temperature,
800 without being able to link the AO influence to known mech-
801 anisms. In the present study area, the AO summer index

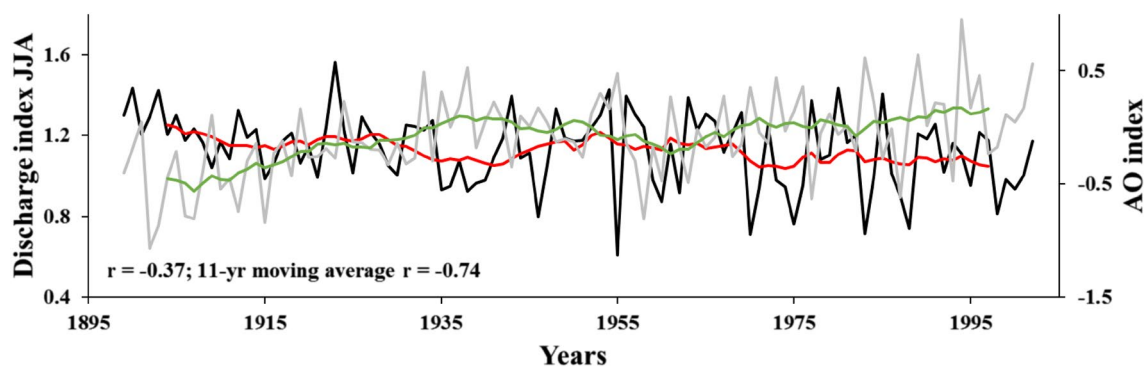


Fig. 6 Summer discharge reconstruction from tree-ring isotopes (black line) inversely correlating with the summer AO index (grey line). Red and green lines represent 11-year moving average for discharge reconstruction and AO index, respectively

802 correlates directly with summer T_{\max} ($r=0.41$; $p<0.05$;
 803 $n=61$), but the AO annual index inversely correlates with
 804 the annual T_{\max} ($r=-0.49$; $p<0.05$; $n=61$). The latter cor-
 805 relation likely reflects the relationship between winter AO
 806 index and winter temperature ($r=-0.63$; $p<0.05$; $n=61$).
 807 The winter AO index also shows low correlation with spring
 808 and summer temperature ($r=-0.14$ and 0.16 , respectively;
 809 $p<0.05$; $n=61$), suggesting a very moderate influence of
 810 AO index on the following seasons. Those observations
 811 suggest that various mechanisms play within the year to
 812 modulate the relationship between AO and temperature. As
 813 shown previously, the winter AO index relationship with
 814 winter conditions is well understood in northeastern Canada,
 815 whereas the summer AO index influence on summer condi-
 816 tions is barely documented. The present study underlines this
 817 influence of summer AO on low and mid-frequency varia-
 818 tions of the reconstructed summer regional discharge, likely
 819 operating through AO's effects on summer regional climatic
 820 conditions. Indeed, further investigations are required to
 821 determine the mechanisms at play for AO to regulate sum-
 822 mer river discharge in eastern Labrador.

823 5 Conclusion

824 This study confirms that the approach used in this research
 825 is one of the most relevant tools to document the variabil-
 826 ity of past hydroclimatic conditions in the northeastern
 827 boreal forest where water availability is not constraining
 828 the growth of trees. The statistical examination suggests
 829 that summer T_{\max} , P_{total} and VPD are the main drivers of
 830 the $\delta^{13}\text{C}$ and $\delta^{18}\text{O}$, and regional discharge variations, and
 831 expresses an indirect link between the isotopic series and
 832 the discharge in the studied region. In addition, evapotran-
 833 spiration partly contributes directly to linking tree-ring
 834 isotopic attributes to water discharge. Hence, tree-ring stable
 835 isotopes can serve for reconstructing summer regional

836 discharge. Moreover, the significant correlation between
 837 reconstructions from tree-ring isotopes and the independ-
 838 ent ANATEM method validates the two approaches. The
 839 reconstructions suggest that this part of Canada has experi-
 840 enced an overall decrease in summer discharge over the
 841 past 200 years. The summer AO is inferred to affect low
 842 and mid-frequency variations of summer regional climatic
 843 conditions in this region. Future research should examine
 844 potential mechanisms by which summer AO index oper-
 845 ates to regulate summer climatic conditions and regional
 846 discharge.

Acknowledgements The authors would like to thank Anna Smirnoff
 847 for technical support in the Delta-Lab at the Geological Survey of
 848 Canada, Québec city, and Pierre Masselot (INRS-ETE) for his help
 849 when converting Matlab code to R code for the $\delta^{13}\text{C}$ PIN correction.
 850 This research was financially supported by the Climate Change Geo-
 851 science program (EXTREME events project) of Natural Resources
 852 Canada (Geological Survey of Canada), NSERC and the OURANOS
 853 consortium through a Collaborative Research and Development Grant
 854 (ARCHIVES project). Support for the twentieth Century Reanaly-
 855 sis Project version 2c dataset was provided by the US Department
 856 of Energy, Office of Science Biological and Environmental Research
 857 (BER), and by the National Oceanic and Atmospheric Administration
 858 Climate Program Office. The production of this manuscript benefitted
 859 from a constructive pre-submission review by Pierre Francus. GSC
 860 contribution number:
 861

862 References

- 863 Allen RG, Pereira LS, Raes D, Smith M (1990) FAO irrigation and
 864 drainage paper no. 56 Crop evapotranspiration (guidelines for
 865 computing crop water requirements)
 866 Alvarez C, Dinis L, Bégin C, Savard MM, Marion J, Smirnoff A, Bégin
 867 Y (2018) Relevance of using whole-ring stable isotopes of black
 868 spruce trees in the perspective of climate reconstruction. *Den-
 869 drochronologia*. <https://doi.org/10.1016/j.dendro.2018.05.004>
 870 Anctil F, Coulibaly P (2004) Wavelet analysis of the interannual
 871 variability in southern Québec streamflow. *J Clim* 17:163–173.
 872 [https://doi.org/10.1175/1520-0442\(2004\)017%3C0163:WAOTI%3E2.0.CO;2](https://doi.org/10.1175/1520-0442(2004)017%3C0163:WAOTI%3E2.0.CO;2)
 873

- 874 Anderson WT, Bernasconi SM, McKenzie JA, Saurer M, Schwein-
875 gruber F (2002) Model evaluation for reconstructing the oxygen
876 isotopic composition in precipitation from tree ring cellulose
877 over the last century. *Chem Geol* 182:121–137. [https://doi.
878 org/10.1016/S0009-2541\(01\)00285-6](https://doi.org/10.1016/S0009-2541(01)00285-6)
- 879 Asong ZE, Wheeler HS, Bonsal B, Razavi S, Kurkute S (2018) Historical
880 drought patterns over Canada and their teleconnections with
881 large-scale climate signals. *Hydrol Earth Syst Sci* 22:3105–3124.
882 <https://doi.org/10.5194/hess-22-3105-2018>
- 883 Axelson JN, Sauchyn DJ, Barichivich J (2009) New reconstructions of
884 streamflow variability in the South Saskatchewan River Basin
885 from a network of tree ring chronologies, Alberta, Canada. *Water*
886 *Resour Res*. <https://doi.org/10.1029/2008WR007639>
- 887 Barbour MM (2007) Stable oxygen isotope composition of plant tissue:
888 a review. *Funct Plant Biol* 34:83–94. [https://doi.org/10.1071/
889 FP06228](https://doi.org/10.1071/FP06228)
- 890 Bégin C, Filion L (1988) Age of landslides along the Grande
891 Rivière de la Baleine estuary, eastern coast of Hudson
892 Bay, Québec (Canada). *Boreas* 17:289–299. [https://doi.
893 org/10.1111/j.1502-3885.1988.tb00959.x](https://doi.org/10.1111/j.1502-3885.1988.tb00959.x)
- 894 Bégin C, Gingras M, Savard MM, Marion J, Nicault A, Bégin Y (2015)
895 Assessing tree-ring carbon and oxygen stable isotopes for climate
896 reconstruction in the Canadian northeastern boreal forest. *Palaeogeogr Palaeoclimatol Palaeoecol* 423:91–101. [https://doi.
897 org/10.1016/j.palaeo.2015.01.021](https://doi.org/10.1016/j.palaeo.2015.01.021)
- 898 Begueria S, Latorre B, Reig F, Vicente-Serrano SM (2018) The stand-
899 ardisised precipitation-evapotranspiration index [WWW Document].
900 <http://spei.csic.es/index.html>
- 901 Betts RA, Boucher O, Collins M, Cox PM, Falloon PD, Gedney N,
902 Hemming DL, Huntingford C, Jones CD, Sexton DMH, Webb
903 MJ (2007) Projected increase in continental runoff due to plant
904 responses to increasing carbon dioxide. *Nature* 448:1037–1041.
905 <https://doi.org/10.1038/nature06045>
- 906 Bhiry N, Delwaide A, Allard M, Bégin Y, Filion L, Lavoie M, Nozais
907 C, Payette S, Pienitz R, Saulnier-Talbot É, Vincent WF (2011)
908 Environmental change in the Great Whale River region, Hud-
909 son Bay: five decades of multidisciplinary research by Centre
910 d'études nordiques (CEN). *Écoscience* 18:182–203. [https://doi.
911 org/10.2980/18-3-3469](https://doi.org/10.2980/18-3-3469)
- 912 Blais JR (1962) Collection and analysis of radial-growth data from
913 trees for evidence of past spruce budworm outbreaks. *For Chron*
914 38:474–484. <https://doi.org/10.5558/tfc38474-4>
- 915 Bonsal B, Shabbar A (2008) Impacts of large-scale circulation variability
916 on low streamflows over Canada: a review. *Can Water Resour*
917 *J Rev Can Ressour Hydr* 33:137–154. [https://doi.org/10.4296/
918 cwrj3302137](https://doi.org/10.4296/cwrj3302137)
- 919 Borella S, Leuenberger M, Saurer M, Siegwolf RTW (1998) Reducing
920 uncertainties in $\delta^{13}\text{C}$ analysis of tree rings: pooling, milling, and
921 cellulose extraction. *J Geophys Res Atmos* 103:19519–19526.
922 <https://doi.org/10.1029/98JD01169>
- 923 Boucher E, Nicault A, Arseneault D, Bégin Y, Karami MP (2017)
924 Decadal variations in eastern Canada's taiga wood biomass
925 production forced by ocean-atmosphere interactions. *Sci Rep*
926 7:2457. <https://doi.org/10.1038/s41598-017-02580-9>
- 927 Boulanger Y, Arseneault D (2004) Spruce budworm outbreaks in
928 eastern Quebec over the last 450 years. *Can J For Res* 34:1035–
929 1043. <https://doi.org/10.1139/x03-269>
- 930 Brien RJW, Gloor E, Clerici S, Newton R, Arppe L, Boom A, Bot-
931 trell S, Callaghan M, Heaton T, Helama S, Helle G, Leng MJ,
932 Mielikäinen K, Oinonen M, Timonen M (2017) Tree height
933 strongly affects estimates of water-use efficiency responses to
934 climate and CO_2 using isotopes. *Nat Commun* 8:288. [https://
935 doi.org/10.1038/s41467-017-00225-z](https://doi.org/10.1038/s41467-017-00225-z)
- 936 Briffa KR, Jones PD, Pilcher JR, Hughes MK (1988) Reconstructing
937 summer temperatures in northern Fennoscandia back to
938 AD 1700 using tree-ring data from Scots pine. *Arct Alp Res* 20:385–394. <https://doi.org/10.2307/1551336>
- 939 Brigode P, Brissette F, Nicault A, Perreault L, Kuentz A, Mathevet T,
940 Gailhard J (2016) Streamflow variability over the 1881–2011
941 period in northern Québec: comparison of hydrological recon-
942 structions based on tree rings and geopotential height field
943 reanalysis. *Clim Past* 12:1785–1804. [https://doi.org/10.5194/
944 cp-12-1785-2016](https://doi.org/10.5194/cp-12-1785-2016)
- 945 Buermann W, Anderson B, Tucker CJ, Dickinson RE, Lucht W, Pot-
946 ter CS, Myneni RB (2003) Interannual covariability in North-
947 ern Hemisphere air temperatures and greenness associated
948 with El Niño-Southern Oscillation and the Arctic Oscillation.
949 *J Geophys Res Atmos*. <https://doi.org/10.1029/2002JD002630>
- 950 Buras A (2017) A comment on the expressed population signal.
951 *Dendrochronologia* 44:130–132. [https://doi.org/10.1016/j.
952 dendro.2017.03.005](https://doi.org/10.1016/j.dendro.2017.03.005)
- 953 Cao L, Bala G, Caldeira K, Nemani R, Ban-Weiss G (2010) Import-
954 ance of carbon dioxide physiological forcing to future cli-
955 mate change. *Proc Natl Acad Sci* 107:9513–9518. [https://doi.
956 org/10.1073/pnas.0913000107](https://doi.org/10.1073/pnas.0913000107)
- 957 Case RA, MacDonald GM (2003) Tree ring reconstruc-
958 tions of streamflow for three Canadian Prairie riv-
959 ers. *J Am Water Resour Assoc* 39:703–716. [https://doi.
960 org/10.1111/j.1752-1688.2003.tb03686.x](https://doi.org/10.1111/j.1752-1688.2003.tb03686.x)
- 961 Cho M-H, Lim G-H, Song H-J (2014) The effect of the wintertime
962 Arctic Oscillation on springtime vegetation over the northern
963 high latitude region. *Asia Pac J Atmos Sci* 50:567–573. [https://
964 doi.org/10.1007/s13143-014-0046-1](https://doi.org/10.1007/s13143-014-0046-1)
- 965 Clark ID, Fritz P (1997) Environmental isotopes in hydrogeology. CRC
966 Press, Boca Raton
- 967 Cohen S, Koshida G, Mortsch L (2015) Climate and water availability
968 indicators in Canada: challenges and a way forward. Part III—
969 future scenarios. *Can Water Resour J* 40:160–172. [https://doi.
970 org/10.1080/07011784.2015.1006021](https://doi.org/10.1080/07011784.2015.1006021)
- 971 Compo GP, Whitaker JS, Sardeshmukh PD, Matsui N, Allan RJ, Yin X,
972 Gleason BE, Vose RS, Rutledge G, Bessemoulin P, Brönnimann
973 S, Brunet M, Crouthamel RI, Grant AN, Groisman PY, Jones PD,
974 Kruk MC, Kruger AC, Marshall GJ, Mauerer M, Mok HY, Nordli
975 Ø, Ross TF, Trigo RM, Wang XL, Woodruff SD, Worley SJ
976 (2011) The twentieth century reanalysis project. *Q J R Meteorol*
977 *Soc* 137:1–28. <https://doi.org/10.1002/qj.776>
- 978 Cook ER, Meko DM, Stahle DW, Cleaveland MK (1999) Drought
979 reconstructions for the continental United States. *J Clim* 12:1145–
980 1162. [https://doi.org/10.1175/1520-0442\(1999\)012%3C1145:
981 5:DRFTCU%3E2.0.CO;2](https://doi.org/10.1175/1520-0442(1999)012%3C1145:DRFTCU%3E2.0.CO;2)
- 982 Core Team R (2018) R: the R project for statistical computing [WWW
983 Document]. <https://www.r-project.org/>. Accessed 22 Aug 18
- 984 Coulibaly P, Burn DH (2005) Spatial and temporal variability of
985 Canadian seasonal streamflows. *J Clim* 18:191–210. [https://doi.
986 org/10.1175/JCLI-3258.1](https://doi.org/10.1175/JCLI-3258.1)
- 987 Coulibaly P, Ancil F, Rasmussen P, Bobée B. (2000) A recurrent
988 neural networks approach using indices of low-frequency cli-
989 matic variability to forecast regional annual runoff. *Hydrol Pro-
990 cess* 14:2755–2777. [https://doi.org/10.1002/1099-1085\(20001
991 030\)14:15%3C2755::AID-HYP90%3E3.0.CO;2-9](https://doi.org/10.1002/1099-1085(20001030)14:15%3C2755::AID-HYP90%3E3.0.CO;2-9)
- 992 Coulthard B, Smith DJ (2016) A 477-year dendrohydrological assess-
993 ment of drought severity for Tsable River, Vancouver Island,
994 British Columbia, Canada. *Hydrol Process* 30:1676–1690. <https://doi.org/10.1002/hyp.10726>
- 995 Cram TA, Compo GP, Yin X, Allan RJ, McColl C, Vose RS, Whit-
996 taker JS, Matsui N, Ashcroft L, Auchmann R, Bessemoulin P,
997 Brandsma T, Brohan P, Brunet M, Comeaux J, Crouthamel R,
998 Gleason BE, Groisman PY, Hersbach H, Jones PD, Jönsson T,
999 Jourdain S, Kelly G, Knapp KR, Kruger A, Kubota H, Lentini
1000 G, Lorrey A, Lott N, Lubker SJ, Luterbacher J, Marshall GJ,
1001 Mauerer M, Mock CJ, Mok HY, Nordli Ø, Rodwell MJ, Ross
1002 1003 1004

- TF, Schuster D, Srnec L, Valente MA, Vizi Z, Wang XL, Westcott N, Woollen JS, Worley SJ (2015) The international surface pressure databank version 2. *Geosci Data J* 2:31–46. <https://doi.org/10.1002/gdj3.25>
- Csank AZ, Fortier D, Leavitt SW (2013) Annually resolved temperature reconstructions from a late Pliocene–early Pleistocene polar forest on Bylot Island, Canada. *Palaeogeogr Palaeoclimatol Palaeoecol* 369:313–322. <https://doi.org/10.1016/j.palaeo.2012.10.040>
- D'Arrigo R, Buckley B, Kaplan S, Woollett J (2003) Interannual to multidecadal modes of Labrador climate variability inferred from tree rings. *Clim Dyn* 20:219–228. <https://doi.org/10.1007/s00382-002-0275-3>
- Dansgaard W (1964) Stable isotopes in precipitation. *Tellus* 16:436–468. <https://doi.org/10.1111/j.2153-3490.1964.tb00181.x>
- Daux V, Michelot-Antalik A, Lavergne A, Pierre M, Stievenard M, Bréda N, Damesin C (2018) Comparisons of the performance of $\delta^{13}\text{C}$ and $\delta^{18}\text{O}$ of *Fagus sylvatica*, *Pinus sylvestris*, and *Quercus petraea* in the record of past climate variations. *J Geophys Res Biogeosci* 123:1145–1160. <https://doi.org/10.1002/2017JG004203>
- Déry SJ, Hernández-Henríquez MA, Burford JE, Wood EF (2009) Observational evidence of an intensifying hydrological cycle in northern Canada. *Geophys Res Lett.* <https://doi.org/10.1029/2009GL038852>
- Dobesberger EJ, Lim KP, Raske AG (1983) Spruce budworm (Lepidoptera: Tortricidae) moth flight from New Brunswick to Newfoundland. *Can Entomol* 115:1641–1645. <https://doi.org/10.4039/Ent1151641-12>
- Dorado Liñán I, Gutiérrez E, Helle G, Heinrich I, Andreu-Hayles L, Planells O, Leuenberger M, Bürger C, Schleser G (2011) Pooled versus separate measurements of tree-ring stable isotopes. *Sci Total Environ* 409:2244–2251. <https://doi.org/10.1016/j.scitotenv.2011.02.010>
- Dyke AS, Andrews J, Clark PU, England JH, Miller GH, Shaw J, Veilleux JJ (2002) The Laurentide and Innuitian ice sheets during the last glacial maximum. *Quat Sci Rev* 21:9–31. [https://doi.org/10.1016/S0277-3791\(01\)00095-6](https://doi.org/10.1016/S0277-3791(01)00095-6)
- Elshorbagy A, Wagener T, Razavi S, Sauchyn D (2016) Correlation and causation in tree-ring-based reconstruction of paleohydrology in cold semiarid regions. *Water Resour Res* 52:7053–7069. <https://doi.org/10.1002/2016WR018985>
- Farquhar GD, O'Leary MH, Berry JA (1982) On the relationship between carbon isotope discrimination and the intercellular carbon dioxide concentration in leaves. *Funct Plant Biol* 9:121–137. <https://doi.org/10.1071/pp9820121>
- Farquhar GD, Ehleringer JR, Hubick KT (1989) Carbon isotope discrimination and photosynthesis. *Annu Rev Plant Physiol Plant Mol Biol* 40:503–537. <https://doi.org/10.1146/annurev.pl.40.060189.002443>
- Ferrio JP, Voltas J (2005) Carbon and oxygen isotope ratios in wood constituents of *Pinus halepensis* as indicators of precipitation, temperature and vapour pressure deficit. *Tellus B Chem Phys Meteorol* 57:164–173. <https://doi.org/10.3402/tellusb.v57i2.16780>
- Gagen M, Zorita E, McCarroll D, Young GHF, Grudd H, Jalkanen R, Loader NJ, Robertson I, Kirchhefer A (2011) Cloud response to summer temperatures in Fennoscandia over the last thousand years. *Geophys Res Lett.* <https://doi.org/10.1029/2010GL046216>
- Gazis C, Feng X (2004) A stable isotope study of soil water: evidence for mixing and preferential flow paths. *Geoderma* 119:97–111. [https://doi.org/10.1016/S0016-7061\(03\)00243-X](https://doi.org/10.1016/S0016-7061(03)00243-X)
- Gedney N, Cox PM, Betts RA, Boucher O, Huntingford C, Stott PA (2006) Detection of a direct carbon dioxide effect in continental river runoff records. *Nature* 439:835–838. <https://doi.org/10.1038/nature04504>
- Government of Canada (2018a) Historical hydrometric data search [WWW Document]. https://wateroffice.ec.gc.ca/search/historical_e.html. Accessed 25 May 18
- Government of Canada (2018b) Adjusted and homogenized Canadian climate data (AHCCD) [WWW Document]. <http://www.ec.gc.ca/dcccha-ahccd/>
- Government of Canada (2018c) Regional, national and international climate modeling [WWW Document]. <http://cfs.nrcan.gc.ca/projects/3>
- Government of Newfoundland Labrador (2018a) Electricity [WWW Document]. <http://www.nr.gov.nl.ca/nr/energy/electricity/index.html>. Accessed 24 May 18
- Government of Newfoundland Labrador (2018b) Fisheries and land resources [WWW Document]. <http://www.flr.gov.nl.ca/publications/parks/index.html#other>
- Greene BA (1974) An outline of the geology of Labrador. *J Geol Assoc Can* 1
- Grimard Y, Jones HG (1982) Trophic upsurge in new reservoirs: a model for total phosphorus concentrations. *Can J Fish Aquat Sci* 39:1473–1483. <https://doi.org/10.1139/f82-199>
- Hart SJ, Smith DJ, Clague JJ (2010) A multi-species dendroclimatic reconstruction of Chilko river streamflow, British Columbia, Canada. *Hydrol Process* 24:2752–2761. <https://doi.org/10.1002/hyp.7674>
- Holmes RL (1983) Computer-assisted quality control in tree-ring dating and measurement. *Tree-Ring Bull* 1983:51–67
- Hook BA, Halfar J, Gedalof Z, Bollmann J, Schulze DJ (2015) Stable isotope paleoclimatology of the earliest Eocene using kimberlite-hosted mummified wood from the Canadian Subarctic. *Biogeosciences* 12:5899–5914. <https://doi.org/10.5194/bg-12-5899-2015>
- Hutchinson MF, McKenney DW, Lawrence K, Pedlar JH, Hopkinson RF, Milewska E, Papadopol P (2009) Development and testing of Canada-wide interpolated spatial models of daily minimum–maximum temperature and precipitation for 1961–2003. *J Appl Meteorol Climatol* 48:725–741. <https://doi.org/10.1175/2008JAMC1979.1>
- Jandhyala VK, Liu P, Fotopoulos SB (2009) River stream flows in the northern québec labrador region: a multivariate change point analysis via maximum likelihood. *Water Resour Res.* <https://doi.org/10.1029/2007WR006499>
- Knauer J, Zaehle S, Reichstein M, Medlyn BE, Forkel M, Hagemann S, Werner C (2017) The response of ecosystem water-use efficiency to rising atmospheric CO₂ concentrations: sensitivity and large-scale biogeochemical implications. *New Phytol* 213:1654–1666. <https://doi.org/10.1111/nph.14288>
- Kuentz A, Mathevet T, Gailhard J, Hingray B (2015) Building long-term and high spatio-temporal resolution precipitation and air temperature reanalyses by mixing local observations and global atmospheric reanalyses: the ANATEM model. *Hydrol Earth Syst Sci* 19:2717–2736. <https://doi.org/10.5194/hess-19-2717-2015>
- Leavitt SW (2010) Tree-ring C–H–O isotope variability and sampling. *Sci Total Environ* 408:5244–5253. <https://doi.org/10.1016/j.scitotenv.2010.07.057>
- Leuenberger M (1998) Stable Isotopes in tree rings as climate and stress indicators. vdf Hochschulverlag AG, Zurich
- Liu X, An W, Treydte K, Wang W, Xu G, Zeng X, Wu G, Wang B, Zhang X (2015) Pooled versus separate tree-ring δD measurements, and implications for reconstruction of the Arctic Oscillation in northwestern China. *Sci Total Environ* 511:584–594. <https://doi.org/10.1016/j.scitotenv.2015.01.002>
- Loader NJ, Santillo PM, Woodman-Ralph JP, Rolfe JE, Hall MA, Gagen M, Robertson I, Wilson R, Froyd CA, McCarroll D (2008)

- 1136 Multiple stable isotopes from oak trees in southwestern Scot- 1202
 1137 land and the potential for stable isotope dendroclimatology in 1203
 1138 maritime climatic regions. *Chem Geol Stab Isot Anal Tree Rings* 1204
 1139 252:62–71. <https://doi.org/10.1016/j.chemgeo.2008.01.006> 1205
 1140 Loader NJ, Young GHF, Grudd H, McCarroll D (2013a) Stable carbon 1206
 1141 isotopes from Torneträsk, northern Sweden provide a millen- 1207
 1142 nial length reconstruction of summer sunshine and its relation- 1208
 1143 ship to Arctic circulation. *Quat Sci Rev* 62:97–113. <https://doi.org/10.1016/j.quascirev.2012.11.014> 1209
 1144 Loader NJ, Young GHF, McCarroll D, Wilson RJS (2013b) Quantify- 1210
 1145 ing uncertainty in isotope dendroclimatology. Holocene. <https://doi.org/10.1177/0959683613486945> 1211
 1146 Marshall JD, Monserud RA (2006) Co-occurring species differ in tree- 1212
 1147 ring 18O trends 26, 12 1213
 1148 McCarroll D, Loader NJ (2004) Stable isotopes in tree rings. *Isot Quat* 1214
 1149 *Paleoenvir Reconstr* 23:771–801. <https://doi.org/10.1016/j.quascirev.2003.06.017> 1215
 1150 McCarroll D, Jalkanen R, Hicks S, Tuovinen M, Gagen M, Pawellek F, 1216
 1151 Eckstein D, Schmitt U, Autio J, Heikkinen O (2003) Multiproxy 1217
 1152 dendroclimatology: a pilot study in northern Finland. *Holocene* 1218
 1153 13:829–838. <https://doi.org/10.1191/0959683603hl668rp> 1219
 1154 McCarroll D, Gagen MH, Loader NJ, Robertson I, Anchukaitis KJ, Los 1220
 1155 S, Young GHF, Jalkanen R, Kirchhefer A, Waterhouse JS (2009) 1221
 1156 Correction of tree ring stable carbon isotope chronologies for 1222
 1157 changes in the carbon dioxide content of the atmosphere. *Geochim Cosmochim Acta* 73:1539–1547. <https://doi.org/10.1016/j.gca.2008.11.041> 1223
 1158 Mortsch L, Cohen S, Koshida G (2015) Climate and water availabil- 1224
 1159 ity indicators in Canada: challenges and a way forward. Part 1225
 1160 II—historic trends. *Can Water Resour J Rev Can Ressour Hydr* 1226
 1161 40:146–159. <https://doi.org/10.1080/07011784.2015.1006024> 1227
 1162 Natural Resources Canada (2018) About renewable energy [WWW 1228
 1163 Document]. <https://www.nrcan.gc.ca/energy/renewable-electricity/7295#hydro> 1229
 1164 Naulier M, Savard MM, Bégin C, Marion J, Arseneault D, Bégin Y 1230
 1165 (2014) Carbon and oxygen isotopes of lakeshore black spruce 1231
 1166 trees in northeastern Canada as proxies for climatic reconstruc- 1232
 1167 tion. *Chem Geol* 374–375:37–43. <https://doi.org/10.1016/j.chemgeo.2014.02.031> 1233
 1168 Naulier M, Savard MM, Bégin C, Gennaretti F, Arseneault D, Marion 1234
 1169 J, Nicault A, Bégin Y (2015a) A millennial summer temperature 1235
 1170 reconstruction for northeastern Canada using oxygen isotopes in 1236
 1171 relict trees. *Clim Past* 11:1153–1164. <https://doi.org/10.5194/cp-11-1153-2015> 1237
 1172 Naulier M, Savard MM, Bégin C, Marion J, Nicault A, Bégin Y 1238
 1173 (2015b) Temporal instability of isotopes—climate statistical rela- 1239
 1174 tionships—a study of black spruce trees in northeastern Canada. 1240
 1175 *Dendrochronologia* 34:33–42. <https://doi.org/10.1016/j.dendro.2015.04.001> 1241
 1176 Nealis VG, Régnière J (2004) Insect–host relationships influencing dis- 1242
 1177 turbance by the spruce budworm in a boreal mixedwood forest. 1243
 1178 *Can J For Res* 34:1870–1882. <https://doi.org/10.1139/x04-061> 1244
 1179 Nicault A, Boucher E, Bégin C, Guiot J, Marion J, Perreault L, Roy R, 1245
 1180 Savard MM, Bégin Y (2014) Hydrological reconstruction from 1246
 1181 tree-ring multi-proxies over the last two centuries at the Cania- 1247
 1182 piscou Reservoir, northern Québec, Canada. *J Hydrol* 513:435– 1248
 1183 445. <https://doi.org/10.1016/j.jhydrol.2014.03.054> 1249
 1184 Nishimura PH (2009) Dendroclimatology, dendroecology and climate 1250
 1185 change in western Labrador, Canada (Master). Memorial Uni- 1251
 1186 versity of Newfoundland, Labrador 1252
 1187 Nishimura PH, Laroque CP (2011) Observed continentality in radial 1253
 1188 growth–climate relationships in a twelve site network in west- 1254
 1189 ern Labrador, Canada. *Dendrochronologia* 29:17–23. <https://doi.org/10.1016/j.dendro.2010.08.003> 1255
 1190 Ogi M, Tachibana Y, Yamazaki K (2003) Impact of the winter- 1256
 1191 time North Atlantic Oscillation (NAO) on the summertime 1257
 1192 atmospheric circulation. *Geophys Res Lett.* <https://doi.org/10.1029/2003GL017280> 1258
 1193 Ogi M, Yamazaki K, Tachibana Y (2004) The summertime annular 1259
 1194 mode in the northern hemisphere and its linkage to the win- 1260
 1195 ter mode. *J Geophys Res Atmos.* <https://doi.org/10.1029/2004JD004514> 1261
 1196 Ols C, Trouet V, Girardin MP, Hofgaard A, Bergeron Y, Drobyshev I (2018) Post-1980 shifts in the sensitivity of boreal tree 1262
 1197 growth to North Atlantic Ocean dynamics and seasonal climate. 1263
 1198 *Glob Planet Change* 165:1–12. <https://doi.org/10.1016/j.gloplacha.2018.03.006> 1264
 1199 Payette S, Morneau C, Sirois L, Despons M (1989) Recent fire history 1265
 1200 of the Northern Québec Biomes. *Ecology* 70:656–673. <https://doi.org/10.2307/1940217> 1266
 1201 Porter TJ, Pisaric MFJ, Kokelj SV, Edwards TWD (2009) Climatic 1267
 1202 signals in $\delta^{13}\text{C}$ and $\delta^{18}\text{O}$ of tree-rings from white spruce in the 1268
 1203 Mackenzie Delta Region, Northern Canada. *Arct Antarct Alp* 1269
 1204 *Res* 41:497–505. <https://doi.org/10.1657/1938-4246.41.4.497> 1270
 1205 Porter TJ, Pisaric MFJ, Field RD, Kokelj SV, Edwards TWD, deMontigny P, Healy R, LeGrande AN (2014) Spring–summer tempera- 1271
 1206 tures since AD 1780 reconstructed from stable oxygen 1272
 1207 isotope ratios in white spruce tree-rings from the Mackenzie 1273
 1208 Delta, northwestern Canada. *Clim Dyn* 42:771–785. <https://doi.org/10.1007/s00382-013-1674-3> 1274
 1209 Raske AG, Clarke LJ, Sutton WJ (1986) The status of the spruce bud- 1275
 1210 worm in Newfoundland and Labrador in 1983–1985 1276
 1211 Roberts BA, Simon NPP, Deering KW (2006) The forests and wood- 1277
 1212 lands of Labrador, Canada: ecology, distribution and future man- 1278
 1213 agement. *Ecol Res* 21:868–880. <https://doi.org/10.1007/s12184-006-0051-7> 1279
 1214 Roberts J, Pryse-Phillips A, Snelgrove K (2012) Modeling the potential 1280
 1215 impacts of climate change on a small watershed in Labrador, 1281
 1216 Canada. *Can Water Resour J Rev Can Ressour Hydr* 37:231–251. 1282
 1217 <https://doi.org/10.4296/cwrj2011-923> 1283
 1218 Robichaud B, Mullock J (2001) The weather of Atlantic Canada and 1284
 1219 eastern Quebec 1285
 1220 Roden JS, Lin G, Ehleringer JR (2000) A mechanistic model for inter- 1286
 1221 pretation of hydrogen and oxygen isotope ratios in tree-ring 1287
 1222 cellulose. *Geochim Cosmochim Acta* 64:21–35. [https://doi.org/10.1016/S0016-7037\(99\)00195-7](https://doi.org/10.1016/S0016-7037(99)00195-7) 1288
 1223 Rogers J, McHugh M (2002) On the separability of the North Atlantic 1289
 1224 oscillation and Arctic oscillation. *Clim Dyn* 19:599–608. <https://doi.org/10.1007/s00382-002-0247-7> 1290
 1225 Rohde R, Muller RA, Jacobsen R, Muller E, Perlmutter S, Rosenfeld 1291
 1226 A, Wurtele J, Groom D, Wickham C (2014) A New estimate 1292
 1227 of the average earth surface land temperature spanning 1753 to 1293
 1228 2011. *Geoinform Geostat Overv.* <https://doi.org/10.4172/2327-4581.1000101> 1294
 1229 Rood SB, Samuelson GM, Weber JK, Wywrot KA (2005) Twentieth- 1295
 1230 century decline in streamflows from the hydrographic apex of 1296
 1231 North America. *J Hydrol* 306:215–233. <https://doi.org/10.1016/j.jhydrol.2004.09.010> 1297
 1232 Sauchyn DJ, St-Jacques J-M, Luckman BH (2015) Long-term reliabil- 1298
 1233 ity of the Athabasca River (Alberta, Canada) as the water source 1299
 1234 for oil sands mining. *Proc Natl Acad Sci USA* 112:12621–12626. 1300
 1235 <https://doi.org/10.1073/pnas.1509726112> 1301
 1236 Saurer M, Aellen K, Siegwolf R (1997) Correlating $\delta^{13}\text{C}$ and $\delta^{18}\text{O}$ in 1302
 1237 cellulose of trees. *Plant Cell Environ* 20:1543–1550. <https://doi.org/10.1046/j.1365-3040.1997.d01-53.x> 1303
 1238 Saurer M, Siegwolf RTW, Schweingruber FH (2004) Carbon isotope 1304
 1239 discrimination indicates improving water-use efficiency of trees 1305
 1240 in northern Eurasia over the last 100 years. *Glob Change Biol* 1306
 1241 10:2109–2120. <https://doi.org/10.1111/j.1365-2486.2004.00869.x> 1307
 1242 Scheidegger Y, Saurer M, Bahn M, Siegwolf R (2000) Linking stable 1308
 1243 oxygen and carbon isotopes with stomatal conductance 1309

- 1268 and photosynthetic capacity: a conceptual model. *Oecologia* 125:350–357. <https://doi.org/10.1007/s004420000466>
- 1269 Shabbar A, Skinner W (2004) Summer drought patterns in Can- 1324
1270 ada and the relationship to global sea surface tempera- 1325
1271 tures. *J Clim* 17:2866–2880. [https://doi.org/10.1175/1520-](https://doi.org/10.1175/1520-1326)
1272 [0442\(2004\)017%3C2866:SDPICA%3E2.0.CO;2](https://doi.org/10.1175/1520-0442(2004)017%3C2866:SDPICA%3E2.0.CO;2) 1327
- 1273 Sicre M-A, Weckström K, Seidenkrantz M-S, Kuijpers A, Benetti M, 1328
1274 Masse G, Ezat U, Schmidt S, Bouloubassi I, Olsen J, Khodri M, 1329
1275 Mignot J (2014) Labrador current variability over the last 2000 1330
1276 years. *Earth Planet Sci Lett* 400:26–32. [https://doi.org/10.1016/j.](https://doi.org/10.1016/j.epsl.2014.05.016)
1277 [epsl.2014.05.016](https://doi.org/10.1016/j.epsl.2014.05.016) 1331
- 1278 Simard S, Elhani S, Morin H, Krause C, Cherubini P (2008) Carbon 1332
1279 and oxygen stable isotopes from tree-rings to identify spruce 1333
1280 budworm outbreaks in the boreal forest of Québec. *Chem Geol* 1334
1281 *Stab Isot Anal Tree Rings* 252:80–87. [https://doi.org/10.1016/j.](https://doi.org/10.1016/j.chemgeo.2008.01.018)
1282 [chemgeo.2008.01.018](https://doi.org/10.1016/j.chemgeo.2008.01.018) 1335
- 1283 Simard S, Morin H, Krause C, Buhay WM, Treydte K (2012) Tree- 1336
1284 ring widths and isotopes of artificially defoliated balsam firs: 1337
1285 a simulation of spruce budworm outbreaks in Eastern Canada. 1338
1286 *Environ Exp Bot* 81:44–54. [https://doi.org/10.1016/j.](https://doi.org/10.1016/j.envexpbot.2012.02.012)
1287 [envexpbot.2012.02.012](https://doi.org/10.1016/j.envexpbot.2012.02.012) 1339
- 1288 St. George S (2007) Streamflow in the Winnipeg River basin, Canada: 1340
1289 trends, extremes and climate linkages. *J Hydrol* 332:396–411. 1341
1290 <https://doi.org/10.1016/j.jhydrol.2006.07.014> 1342
- 1291 Stockton CW, Fritts HC (1973) Long-term reconstruction of 1343
1292 water level changes for lake Athabasca by analysis of tree. 1344
1293 *JAWRA J Am Water Resour Assoc* 9:1006–1027. [https://doi.](https://doi.org/10.1111/j.1752-1688.1973.tb05826.x)
1294 [org/10.1111/j.1752-1688.1973.tb05826.x](https://doi.org/10.1111/j.1752-1688.1973.tb05826.x) 1345
- 1295 Sullivan PF, Pattison RR, Brownlee AH, Cahoon SMP, Hollingsworth 1346
1296 TN (2016) Effect of tree-ring detrending method on apparent 1347
1297 growth trends of black and white spruce in interior Alaska. *Environ* 1348
1298 *Res Lett*. <https://doi.org/10.1088/1748-9326/11/11/114007> 1349
- 1299 Sveinsson Oli GB, Upmanu L, Vincent F, Luc P, Jocelyn G, Steve 1350
1300 Z, Yochanan K (2008) Forecasting spring reservoir inflows in 1351
1301 Churchill Falls basin in Québec, Canada. *J Hydrol Eng* 13:426– 1352
1302 437. [https://doi.org/10.1061/\(ASCE\)1084-0699\(2008\)13:6\(426\)](https://doi.org/10.1061/(ASCE)1084-0699(2008)13:6(426)) 1353
- 1303 Szymczak S, Joachimski MM, Bräuning A, Hetzer T, Kuhlemann J 1354
1304 (2012) Are pooled tree ring $\delta^{13}C$ and $\delta^{18}O$ series reliable cli- 1355
1305 mate archives? A case study of *Pinus nigra* spp. laricio (Corsica/ 1356
1306 France). *Chem Geol* 308–309:40–49. [https://doi.org/10.1016/j.](https://doi.org/10.1016/j.chemgeo.2012.03.013)
1307 [chemgeo.2012.03.013](https://doi.org/10.1016/j.chemgeo.2012.03.013) 1357
- 1308 Thompson DWJ, Wallace JM (1998) The Arctic oscillation signature in 1358
1309 the wintertime geopotential height and temperature fields. *Geophys* 1359
1310 *Res Lett* 25:1297–1300. [https://doi.org/10.1029/98GL0](https://doi.org/10.1029/98GL00950)
1311 [0950](https://doi.org/10.1029/98GL00950) 1360
- 1312 Thompson DWJ, Wallace JM (2000) Annular modes in the extratropical 1361
1313 circulation. Part I: month-to-month variability. *J Clim* 13:1000– 1362
1314 1016. [https://doi.org/10.1175/1520-0442\(2000\)013%3C1000-](https://doi.org/10.1175/1520-0442(2000)013%3C1000:AMITEC%3E2.0.CO;2)
1315 [0:AMITEC%3E2.0.CO;2](https://doi.org/10.1175/1520-0442(2000)013%3C1000:AMITEC%3E2.0.CO;2) 1363
- 1316 Thompson DWJ, Wallace JM (2001) Regional climate impacts of the 1364
1317 northern hemisphere annular mode. *Science* 293:85–89. <https://doi.org/10.1126/science.1058958> 1365
- 1318 Tremblay L, Larocque M, Anctil F, Rivard C (2011) Teleconnec- 1366
1319 tions and interannual variability in Canadian groundwater 1367
1320 levels. *J Hydrol* 410:178–188. [https://doi.org/10.1016/j.jhydr](https://doi.org/10.1016/j.jhydrol.2011.09.013)
1321 [ol.2011.09.013](https://doi.org/10.1016/j.jhydrol.2011.09.013) 1368
- 1322 Treydte K, Schleser GH, Schweingruber FH, Winiger M (2001) The 1369
1323 climatic significance of $\delta^{13}C$ in subalpine spruces (Lötschental, 1370
1324 Swiss Alps). *Tellus B Chem Phys Meteorol* 53:593–611. [https://](https://doi.org/10.3402/tellusb.v53i5.16639)
1325 doi.org/10.3402/tellusb.v53i5.16639 1371
- 1326 Treydte KS, Schleser GH, Helle G, Frank DC, Winiger M, Haug GH, 1372
1327 Esper J (2006) The twentieth century was the wettest period in 1373
1328 northern Pakistan over the past millennium. *Nature* 440:1179– 1374
1329 1182. <https://doi.org/10.1038/nature04743> 1375
- 1330 Trindade M, Bell T, Laroque CP (2011a) Changing climatic sensitivi- 1376
1331 ties of two spruce species across a moisture gradient in North- 1377
1332 eastern Canada. *Dendrochronologia*, Special issue: papers from 1378
1333 the annual meeting of the Canadian Association of Geographers, 1379
1334 Quebec City, Quebec, May 2008, vol 29, pp 25–30. [https://doi.](https://doi.org/10.1016/j.dendro.2010.10.002)
1335 [org/10.1016/j.dendro.2010.10.002](https://doi.org/10.1016/j.dendro.2010.10.002) 1380
- 1336 Trindade M, Bell T, Laroque CP, Jacobs JD, Hermanutz L (2011b) 1381
1337 Dendroclimatic response of a coastal alpine treeline ecotone: a 1382
1338 multispecies perspective from Labrador. This article is a contri- 1383
1339 bution to the series tree recruitment, growth, and distribution at 1384
1340 the circumpolar forest–tundra transition. *Can J For Res* 41:469– 1385
1341 478. <https://doi.org/10.1139/X10-192> 1386
- 1342 Wang S, Yang Y, Luo Y, Rivera A (2013) Spatial and seasonal 1387
1343 variations in evapotranspiration over Canada’s landmass. 1388
1344 *Hydrol Earth Syst Sci* 17:3561–3575. [https://doi.org/10.5194/](https://doi.org/10.5194/hess-17-3561-2013)
1345 [hess-17-3561-2013](https://doi.org/10.5194/hess-17-3561-2013) 1389
- 1346 Waterhouse JS, Barker AC, Carter AHC, Agafonov LI, Loader NJ 1390
1347 (2000) Stable carbon isotopes in scots pine tree rings preserve a 1391
1348 record of flow of the river Ob. *Geophys Res Lett* 27:3529–3532. 1392
1349 <https://doi.org/10.1029/2000GL006106> 1393
- 1350 Wershaw RL, Friedman I, Heller SJ (1966) Hydrogen isotopic fraction- 1394
1351 ation of water passing through trees. *Adv Org Geochem*. [https://](https://doi.org/10.1016/B978-0-08-012758-3.50007-4)
1352 doi.org/10.1016/B978-0-08-012758-3.50007-4 1395
- 1353 Wigley TML, Briffa KR, Jones PD (1984) On the average value of 1396
1354 correlated time series, with applications in dendroclimatology 1397
1355 and hydrometeorology. *J Clim Appl Meteorol* 23:201–213. 1398
1356 [https://doi.org/10.1175/1520-0450\(1984\)023%3C0201:otavoc%](https://doi.org/10.1175/1520-0450(1984)023%3C0201:otavoc%3E2.0.co;2)
1357 [3E2.0.co;2](https://doi.org/10.1175/1520-0450(1984)023%3C0201:otavoc%3E2.0.co;2) 1399
- 1358 Wils THG, Robertson I, Eshetu Z, Koprowski M, Sass-Klaassen UGW, 1400
1359 Touchan R, Loader NJ (2010) Towards a reconstruction of Blue 1401
1360 Nile baseflow from Ethiopian tree rings. *Holocene* 20:837–848. 1402
1361 <https://doi.org/10.1177/0959683610365940> 1403
- 1362 Woodhouse CA, Lukas JJ (2006) Multi-century tree-ring reconstruc- 1404
1363 tions of colorado streamflow for water resource planning. *Clim* 1405
1364 *Change* 78:293–315. <https://doi.org/10.1007/s10584-006-9055-0> 1406
- 1365 Woodley EJ, Loader NJ, McCarroll D, Young GHF, Robertson I, Hea- 1407
1366 ton THE, Gagen MH (2012) Estimating uncertainty in pooled 1408
1367 stable isotope time-series from tree-rings. *Chem Geol* 294– 1409
1368 295:243–248. <https://doi.org/10.1016/j.chemgeo.2011.12.008> 1410
- 1369 Zhang X, Harvey KD, Hogg WD, Yuzyk TR (2001) Trends in Cana- 1411
1370 dian streamflow. *Water Resour Res* 37:987–998. [https://doi.](https://doi.org/10.1029/2000WR900357)
1371 [org/10.1029/2000WR900357](https://doi.org/10.1029/2000WR900357) 1412

Publisher’s Note Springer Nature remains neutral with regard to jurisdictional claims in published maps and institutional affiliations.

Journal:	382
Article:	4731

Author Query Form

Please ensure you fill out your response to the queries raised below and return this form along with your corrections

Dear Author

During the process of typesetting your article, the following queries have arisen. Please check your typeset proof carefully against the queries listed below and mark the necessary changes either directly on the proof/online grid or in the 'Author's response' area provided below

Query	Details Required	Author's Response
AQ1	Author: Kindly check and confirm the word 'Selected periods' changed to 'Selected bold periods' in Table 1 footer.	
AQ2	Author: Kindly provide the accessed date for Begueria et al. (2018), Government of Canada (2018b, c), Government of Newfoundland Labrador (2018b), Natural Resources Canada (2018).	
AQ3	Author: Kindly provide the page range for Greene (1974).	
AQ4	Author: Kindly provide the complete details for Robichaud and Mullock (2001), Raske et al. (1986), Marshall and Monserud (2006).	